



# ORGANIC CHEMISTRY

---

## FRONTIERS



Cite this: *Org. Chem. Front.*, 2022, **9**, 481

Received 17th September 2021,  
Accepted 15th October 2021  
DOI: 10.1039/d1qo01324f  
[rsc.li/frontiers-organic](http://rsc.li/frontiers-organic)

## Derivatization based on tetrazine scaffolds: synthesis of tetrazine derivatives and their biomedical applications

Hongbao Sun,<sup>1</sup> Qinghe Xue,<sup>a</sup> Chang Zhang,<sup>a</sup> Haoxing Wu,<sup>1</sup> \*<sup>a</sup> and Ping Feng<sup>b</sup>

Bioorthogonal chemistry is widely used in biological systems and has been trialed in patients, attracting a lot of attention in this century. Tetrazine-based bioorthogonal reactions are essential in chemical biology applications, including cellular labeling, live-cell imaging, diagnosis, drug release, and oncotherapy, due to their tunable rapid reaction kinetics and unique fluorogenic characteristics. However, the scope of *de novo* tetrazine synthesis is restricted due to the limited supply of commercial starting materials. Therefore, derivatization based on tetrazine scaffolds has been used to synthesize various tetrazine derivatives to enhance the applications of tetrazine bioorthogonal reactions. Herein, the recent advances in tetrazine scaffold-based derivatizations, including tetrazine skeletons, aromatic substituents and alkyl substituents of tetrazines, have been summarized. The advantages and limitations of the derivatization methods and applications of the developed tetrazine derivatives in bioorthogonal chemistry have also been highlighted.

## 1. Introduction

Bioorthogonal reactions, such as the Staudinger ligation, strain-promoted azide–alkyne cycloaddition (SPAAC), strain-promoted alkyne–nitroso cycloaddition (SPANC), photoclick 1,3-dipolar cycloaddition, and inverse-electron demand Diels–Alder (IEDDA) cycloaddition, have been extensively used in chemical biology and biomedicine studies for imaging, detection and therapy.<sup>1–10</sup> The tetrazine bioorthogonal reactions, including IEDDA reaction with dienophiles<sup>3–6,11,12</sup> and [4 + 1] cycloaddition with isonitriles,<sup>13–16</sup> have attracted more and more attention due to their rapid reaction kinetics and unique fluorescence properties (Fig. 1a and b). According to the latest research progress, the tetrazine involved IEDDA reaction is the most rapid bioorthogonal reaction with fast kinetics (up to  $10^7$  M<sup>-1</sup> s<sup>-1</sup>), and can be used *in vivo* with a nanomolar concentration.<sup>3,17–24</sup> Moreover, it is efficient in drug delivery,<sup>25–33</sup> single-cell detection,<sup>34–37</sup> and immuno-PET imaging.<sup>38–44</sup>

Therefore, it is necessary to develop tetrazine synthesis methods to discover the diversified applications of tetrazine bioorthogonal reactions. Pinner firstly synthesized aromatic

1,2,4,5-tetrazines (*s*-tetrazines) in 1893 *via* a two-step reaction process (condensation of hydrazine and nitrile and the oxidation of dihydrotetrazine) (Fig. 1c).<sup>45</sup> The Pinner synthesis method has been widely used to synthesize aromatic tetrazines, but it is not suitable for aliphatic tetrazines.<sup>46</sup> In recent years, many strategies have been used for tetrazine synthesis due to the development of tetrazine-based bioorthogonal reactions. In 2012, the Devaraj group synthesized symmetrical and unsymmetrical aromatic and aliphatic tetrazines *via* the condensation of nitriles and anhydrous hydrazine using the Lewis acid catalyst Zn(II) or Ni(II) salt.<sup>47</sup> Its widespread use is limited by anhydrous hydrazine. In 2018, the Audebert group developed a sulfur-promoted reaction of nitriles with dichloro-

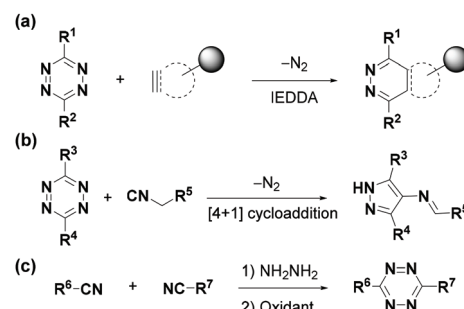


Fig. 1 (a) Bioorthogonal reaction between tetrazine and dienophiles (IEDDA reaction). (b) Bioorthogonal reaction between tetrazine and isonitriles ([4 + 1] cycloaddition). (c) Typical synthesis of the tetrazine skeleton.

<sup>a</sup>Huaxi MR Research Center (HMRRC), Department of Radiology, *Frontiers* Science Center for Disease-related Molecular Network, National Clinical Research Center for Geriatrics, Functional and Molecular Imaging Key Laboratory of Sichuan Province, West China Hospital, Sichuan University, Chengdu 610041, China

<sup>b</sup>Clinical Trial Center, West China Hospital of Sichuan University, Chengdu 610041, China. E-mail: [haoxingwu@scu.edu.cn](mailto:haoxingwu@scu.edu.cn), [fengping@wchscu.cn](mailto:fengping@wchscu.cn)

methane to form monosubstituted aryltetrazines under microwave irradiation using hydrazine hydrate.<sup>48</sup> Recently, the Wu group demonstrated that thiols can promote the reaction between nitriles and hydrazine hydrate to produce unsymmetrical alkyl- or aryl-tetrazine derivatives with good functional group compatibility and satisfactory yields at room temperature.<sup>49</sup> Yet, large amounts of strong oxidants must be used in these methods. Notably, in 2017, the Hu group prepared symmetrical and unsymmetrical dibenzyl-tetrazines through a formal [3 + 3] addition using *gem*-difluoroalkenes and hydrazine hydrate at room temperature with ambient air as the oxidant.<sup>50</sup>

The above *de novo* synthetic strategies were used for constructing tetrazine skeletons. However, most methods use hydrazine, which limits their applications due to its nucleophilicity and reducibility.<sup>6,51</sup> Also, these methods use excessive oxidants, thus limiting the substrate scope. Furthermore, the inadequate commercially available nitriles limit tetrazine synthesis. These limitations hinder the synthesis of tetrazines containing complex functional groups or macromolecules. Therefore, as an alternative strategy, derivatization based on tetrazine scaffolds with substituted tetrazines as building blocks has emerged to produce novel tetrazine derivatives.

Herein, the advances in derivatization based on tetrazine scaffolds since 2014 have been summarized. Three strategies have been discussed: (1) derivatization of tetrazine skeletons; (2) derivatization of alkyl tetrazines; and (3) derivatization of aryl tetrazines. Also, the applications of tetrazine derivatives obtained using these strategies, including bioimaging, drug delivery, detection of DNA and microRNA, and photodynamic therapy, have been highlighted.

## 2. Derivatization of tetrazine skeletons

Chlorotetrazines are synthons that have been widely used due to their high reactivity in nucleophilic aromatic substitution ( $S_NAr$ ) reactions.<sup>46</sup> However,  $S_NAr$  reactions between tetrazines and reactive carbon nucleophiles, such as organo-lithium or Grignard reagents, usually yield nitrogen substitution products.<sup>52</sup> In 2014, the Audebert group prepared six unsymmetrical alkyl-*s*-tetrazines (carbon substitution products, 18–52% yields) *via* an  $S_NAr$  reaction between chlorotetrazines and alkyl lithium reagents.<sup>53</sup> Aromatic halides in electron-deficient systems can undergo both  $S_NAr$  and cross-coupling reactions. Developing cross-coupling reactions under mild conditions can be used to directly synthesize tetrazine derivatives. The Kotschy group reported the first cross-coupling reaction between chlorotetrazines and different terminal alkynes and obtained nine alkynyl tetrazine derivatives in 23–65% yields.<sup>54</sup> Since chlorotetrazines are easily decomposed under coupling reaction conditions, the substrates in this reaction were limited to 6-*N,N*-dialkyl-substituted 3-chlorotetrazines because electron donor groups stabilize tetrazines in the coupling reactions.<sup>54,55</sup> In 2017, the Lindsley group demonstrated that

*N*-alkyl-substituted chlorotetrazines transformed from commercially available 3,6-dichlorotetrazine (7) (Fig. 2a) can be coupled with different aromatic boric acids to obtain high yields (up to 94%) *via* a Suzuki cross-coupling reaction using a BrettPhos Pd G3 catalyst<sup>56</sup> (Fig. 2b). Various unsymmetrical *N*-alkyl-substituted aromatic tetrazines, including tetrazine 15, a derivative of the minaprine analog 16, have been obtained through Suzuki cross-coupling reactions. Tetrazine 15 is an acetylcholinesterase (AChE) inhibitor that can be used as a potential prodrug for senile dementia of the Alzheimer's type (SDAT) with improved drug metabolism and pharmacokinetics (DMPK) properties compared to 16.<sup>57</sup> The electron-donating amino groups on the tetrazines produced by this method decrease their reaction rates during the IEDDA reaction, limiting their application in bioorthogonal chemistry.<sup>3,58</sup>

Besides chlorotetrazines, bromotetrazines are also widely used to synthesize tetrazine derivatives. The Wombacher group<sup>59</sup> used 3-bromo-6-methyl-1,2,4,5-tetrazine (21) (Fig. 3a) for Stille cross-coupling reactions<sup>60</sup> with various tributylstannanes (21–28% yields), followed by further hydrolysis to

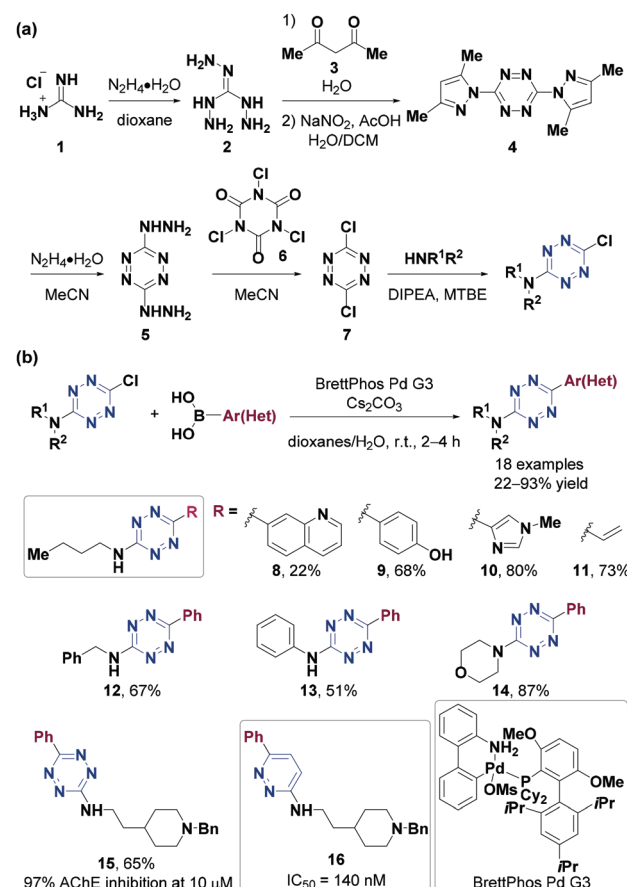
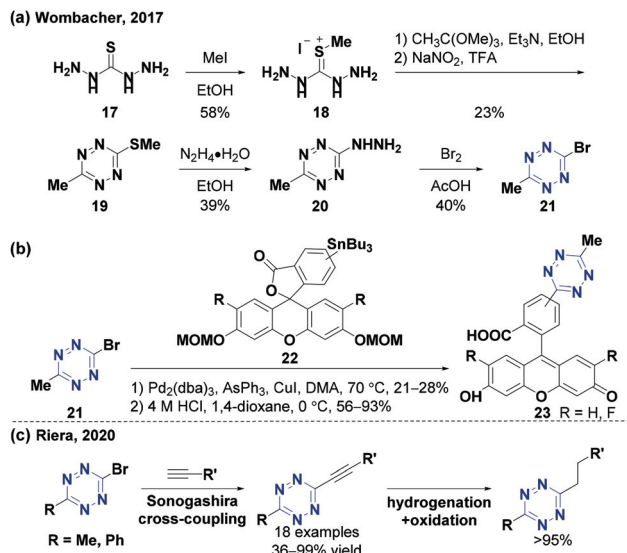


Fig. 2 Synthesis of tetrazine derivatives *via* the Suzuki cross-coupling reaction using chlorotetrazine as the starting building block. (a) Synthesis of *N*-alkyl-substituted chlorotetrazines. (b) Suzuki cross-coupling reaction between *N*-alkyl-substituted chlorotetrazines and aromatic boric acids. DIPEA: *N,N*-diisopropylethylamine, MTBE: methyl *tert*-butyl ether.



**Fig. 3** Synthesis of tetrazine derivatives using 6-substituted bromotetrazines as starting building blocks. (a) Synthesis of 6-methyl bromotetrazine (21) from commercially available thiocarbohydrazide (17). (b) Synthesis of aryltetrazines from a bromotetrazine and a Sn-based reagent *via* Stille cross-coupling. (c) Sonogashira cross-coupling of bromotetrazines and terminal alkynes. OMOM: OMeOMe, TFA: trifluoroacetic acid, and DMA: *N,N*-dimethylacetamide.

generate fluorogenic 3,6-disubstituted tetrazine probes with high water solubility and strong fluorescence enhancement after the IEDDA reaction (Fig. 3b). In 2020, the Riera group<sup>61</sup> synthesized alkynyl-tetrazines (36–99% yields) through Sonogashira-type cross-coupling reactions between bromotetrazines and various terminal alkynes. The alkynyl-tetrazines can undergo hydrogenation, and then oxidation to produce the corresponding alkyl tetrazines in 95–99% yields, thus providing an alternative method for the synthesis of unsymmetrically substituted tetrazines (Fig. 3c).

Many derivatization strategies of tetrazine involve the introduction of an electron-donating group to stabilize the electron-deficient skeleton enhancing coupling reactions. However, tetrazines with 3,6-disubstituted or electron-donating groups are usually less active in IEDDA reactions than those with mono-substituted or electron-withdrawing groups.<sup>3,62</sup> Therefore, 3-monosubstituted tetrazines obtained from 3-bromotetrazine (28) can improve the reaction kinetics. However, a few studies have reported and characterized 3-bromotetrazine (28).<sup>63</sup> In 2020, the Gademann group<sup>64</sup> synthesized and characterized 3-bromotetrazine (28) encouraged by previous reports<sup>65,66</sup> using dibromoiso-cyanuric acid (DBIA) as a bromination agent in the last step (Fig. 4a). 3-Bromotetrazine (28) is a bright orange crystalline solid and a useful precursor for the synthesis of various 3-monosubstituted tetrazines *via* nucleophilic aromatic substitution with suitable bases and solvents, such as 3-phenoxy-s-tetrazine, 3-indole-substituted-s-tetrazine, 3-thiol-s-tetrazine, 3-amino-s-tetrazine, and several tetrazine functional amino acids. 3-Bromotetrazine (28) has been used

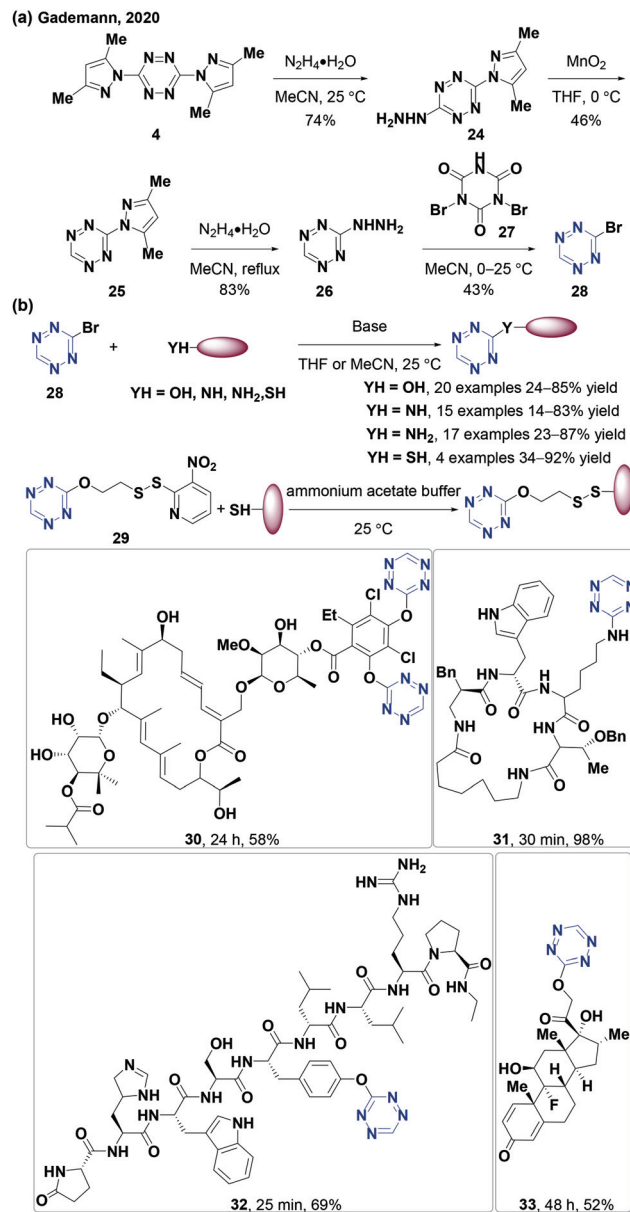


**Fig. 4** Synthesis of tetrazine derivatives using bromotetrazine (28) as the starting building block (part I). (a) Synthesis of bromotetrazine (28) from intermediate 4. (b) Nucleophilic coupling of bromotetrazine (28).

to label macromolecules, including antibiotic fidaxomicin (di-*tet*-fidaxomicin, 30), steroid (*tet*-dexamethasone, 31), and small peptides (tyr(*tet*)-leuprorelin 32 and lys(*tet*)-cycloso-matostatin 33) with excellent selectivity (Fig. 4b). At the same time, the Riera group<sup>67</sup> also synthesized and characterized 3-bromotetrazine (28) using Br<sub>2</sub> as a bromination agent (Fig. 5a). It has been proved to have excellent reactivity in nucleophilic aromatic substitution reactions (Fig. 5b). It was also used for labeling the monoclonal antibody Trastuzumab, which is chemoselective for lysines. The labeled protein can undergo click-to-release bioorthogonal reactions with strained dienophiles to release doxorubicin (Fig. 5c). Recently, the

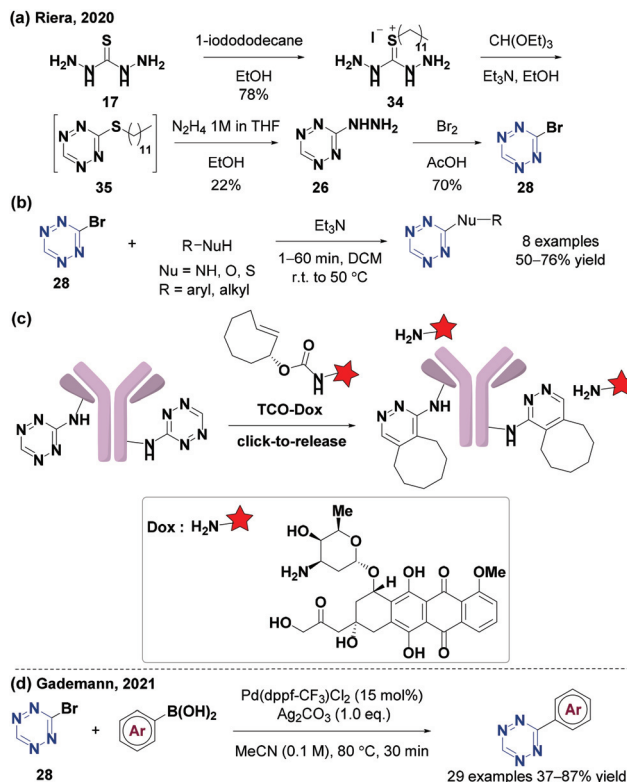


**Fig. 5** Synthesis of tetrazine derivatives using bromotetrazine (28) as the starting building block (part II). (a) Synthesis of bromotetrazine (28) from commercially available thiocarbohydrazide (17). (b) Nucleophilic coupling of bromotetrazine (28). (c) Application in the click-to-release bioorthogonal reaction. (d) Cross-coupling of bromotetrazine with aryl boronic acids.

Gademann group reported the palladium-catalyzed cross-coupling reaction between 3-bromotetrazine (28) and aryl boronic acids using  $\text{Ag}_2\text{CO}_3$  as an activating agent in 37–87% yields with good functional group compatibility<sup>68</sup> (Fig. 5d).

Besides halo-tetrazines, thio-tetrazines are also valuable building blocks that can be used for the synthesis of tetrazine derivatives through aromatic nucleophilic substitution or cross-coupling reactions.<sup>46,55,69</sup> However, the previously reported methods are almost used to synthesize *N*- or *O*-substituted tetrazines with moderate yields. In 2019, the Fox group<sup>70</sup> used 3-thioalkyl tetrazines to synthesize 3-aryl-6-methyl/aryltetrazines through Ag(i)-mediated Liebeskind-Srogl cross-coupling reactions. 3-Thioalkyl tetrazine was obtained *via* a two-step *de novo* synthesis process from a commercially available starting material without using hydrazine (Fig. 6a). In a one-pot operation, thiocarbohydrazide 17 was firstly alkylated with 4-(bromomethyl) biphenyl, and then underwent a condensation reaction with triethyl orthoacetate and Cu-catalyzed oxidation in air, yielding 3-(4'-phenylbenzylthio)-6-methyltetrazine (36) (47% overall yield), a stable and safe crystalline solid (27 g scale) (Fig. 6a). The thio-tetrazines can react with (hetero)arylboronic acids to produce tetrazines through Ag(i)-mediated Liebeskind-Srogl cross-coupling reactions.<sup>71,72</sup>

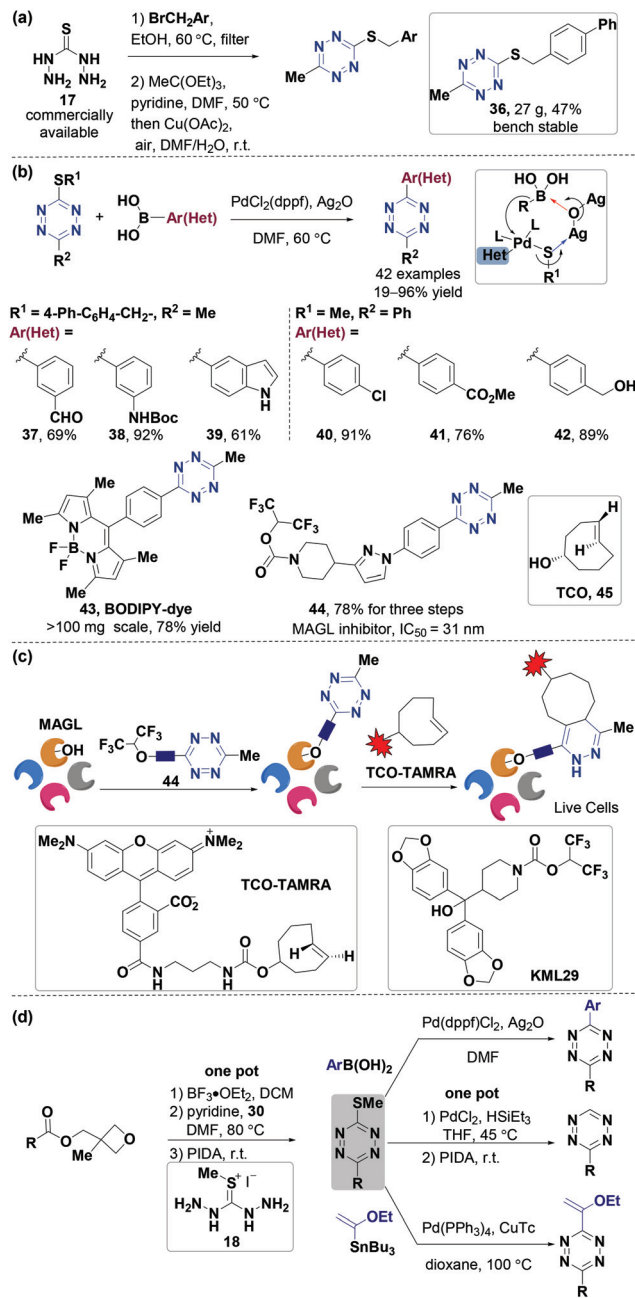


**Fig. 6** Synthesis of tetrazines via derivatization of thio-tetrazines. (a) New strategy for the synthesis of thio-tetrazine on the decagram scale. (b) Synthesis of aryltetrazines with various functional groups through Ag (i)-mediated Liebeskind-Srogl coupling. (c) Selective labeling of endogenous MAGL in human brain vascular pericytes by the tetrazine-functionalized probe 44 and its inhibition by KML29 (experiments were conducted in the presence of TCO-TAMRA). (d) Synthesis of mono-/disubstituted aliphatic or aromatic tetrazines using 3-thiomethyltetrazines from carboxylic esters. PIDA: phenyliodosodiacetate. (c) Adapted from ref. 70 with permission from the American Chemical Society.

Apparently, the combination of a  $\text{PdCl}_2(\text{dppf})$  catalyst with  $\text{Ag}_2\text{O}$  facilitated the coupling reaction between 3-thioalkyl-6-methyltetrazine and (hetero)arylboronic acids, influencing functional group tolerance which could be much broader

under mild conditions, yielding 19–96% (Fig. 6b). This method promotes the derivatization of tetrazine analogs *via* new synthetic routes without using hydrazine. For instance, a boron dipyrromethene (BODIPY)-tetrazine conjugate (**43**) was generated *via* this approach in 78% yield which was much higher than the 8% yield of the conventional hydrazine-based synthesis method<sup>73</sup> (Fig. 6b). Some useful pharmacodynamic groups can be quickly and simply linked with the tetrazine skeleton *via* this method to develop new probes for further applications in the diagnosis and treatment of diseases. For instance, probe **44**, an inhibitor of monoacylglycerol lipase (MAGL), was obtained in 78% yield within three steps. The second-order rate constant of the IEDDA reaction between probe **44** and axial 5-hydroxy-*trans*-cyclooctene (**45**) in methanol at 25 °C is 20.66 M<sup>-1</sup> s<sup>-1</sup>, similar to that of 3-methyl-6-(4-aminomethyl ethyl) tetrazine (19.5 M<sup>-1</sup> s<sup>-1</sup>).<sup>18,74</sup> Furthermore, it was found that probe **44** can inhibit MAGL (IC<sub>50</sub> = 31 nM)<sup>75</sup> *in vitro* and selectively label endogenous MAGL in live cells of human brain vascular pericytes after the IEDDA reaction with TCO-TAMRA (Fig. 6c). This labeling occurred with an IC<sub>50</sub> of 8 nM and was inhibited by the KML29, a MAGL inhibitor,<sup>76</sup> thereby further proving that **44** was a MAGL inhibitor. This synthesis strategy was mainly used to prepare methyl or phenyl unsymmetrical 3,6-disubstituted tetrazines, but it cannot be used to prepare monosubstituted tetrazines. In 2020, the Fox group<sup>77</sup> took a large step in this direction. They used easily synthesized (3-methyloxetan-3-yl)methyl carboxylic esters to obtain 3-thiomethyltetrazines *via* a one-pot method. The method can be used to synthesize mono-/di-substituted aliphatic or aromatic tetrazines through Pd-catalyzed cross-coupling and thioether reduction reactions (Fig. 6d). This strategy uses commercially available carboxyl compounds as starting materials, greatly increasing the range of substrates, and can be used to develop tetrazine probes for chemical biology applications.

The substantial progress in tetrazine skeleton derivatizations for the generation of mono- and di-substituted tetrazines was discussed above. Nevertheless, the unique characteristics of a multi-nitrogen heterocycle tetrazine skeleton with strong electron deficiency limit the type of reaction and the scope of substrates, which cannot meet the huge demands for tetrazines in chemical biology. Therefore, more derivatization strategies are needed.

### 3. Derivatization of alkyl tetrazines

Alkyl tetrazines can be modified through elimination-Heck cascade reactions, Horner–Wadsworth–Emmons (HWE) reactions, and hydrogenation reactions of alkenyl- and alkynyl-tetrazines to directly prepare tetrazine derivatives for chemical biology applications.

In 2014, the Devaraj group<sup>78</sup> synthesized the π-conjugated tetrazine derivatives (*E*)-3-substituted-6-alkenyl-1,2,4,5-tetrazines. They developed a new class of tetrazine building blocks, 3-substituted 6-mesyloxyethyl-tetrazines, which were stable

and can be easily synthesized. These compounds can react with a variety of aryl halides through a Pd-catalyzed *in situ* elimination-Heck cascade reaction to obtain a series of π-conjugated 1,2,4,5-tetrazine derivatives (Fig. 7a), indicating feasible conditions for Pd-catalyzed reactions involving tetrazine. In the same way, utilization of alternative vinyl-tetrazine precursors generated several 3-substituted alkyl-tetrazine analogues, including the Boc-protected amine alkyl tetrazine **47** in 91% yield, as well as diverse alkyl-tetrazines bearing bulky, electron-donating, electron-withdrawing, or heterocyclic substituents in excellent yields (Fig. 7a). This strategy also provided a synthesis route for longer conjugated buta-1,3-diene-substituted tetrazines, such as bistyryl- and diphenylbutadiene-substituted *s*-tetrazines (**48** and **49**), which had never been synthesized before. Compounds **50** and **51** were also synthesized with moderate yields under optimized elimination-Heck reaction conditions, and can be deprotected to obtain tetrazine-modified amino acid and nucleoside derivatives. Three new fluorescent probes were developed by coupling tetrazine with different fluorescent precursors: tetrazine-conjugated BODIPY **52**, rhodamine **53** and difluoro-fluorescein (Oregon-Green) **54**. These probes showed up to 400-fold fluorescence enhancement upon reaction with *trans*-cyclooct-4-

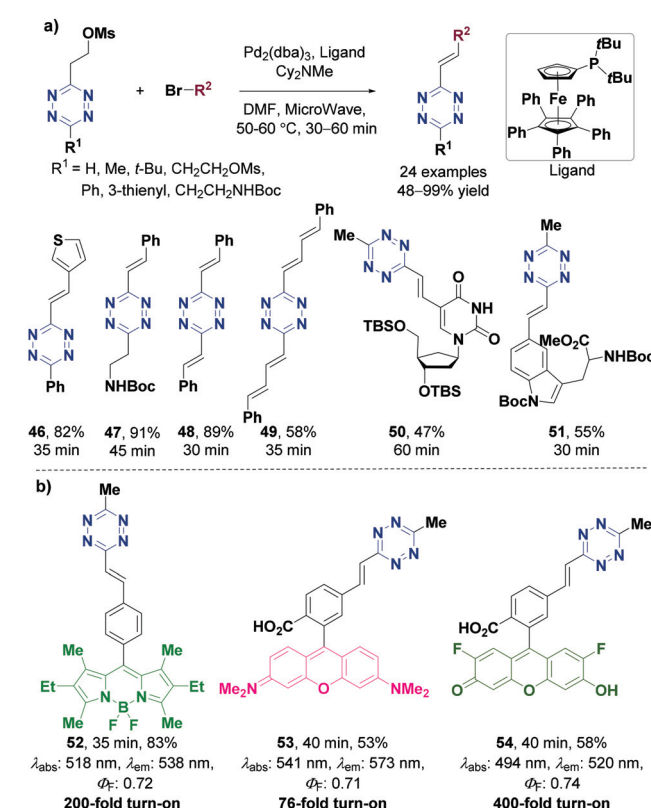


Fig. 7 *In situ* synthesis of alkenyl-tetrazines. (a) Synthesis of π-conjugated tetrazine derivatives through an elimination-Heck cascade reaction. (b) Structures of the tetrazine-conjugated BODIPY **52** and xanthene dyes (rhodamine **53** and difluoro-fluorescein (Oregon-Green) **54**) and their strong emissions after reaction with *trans*-cyclooct-4-enol (TCO).

enol (TCO) with high quantum yields (Fig. 7b). Furthermore, these alkanyl-tetrazines could be transferred to dialkyl-tetrazines through hydrogenation and oxidation. Therefore, this strategy is essential in tetrazine chemistry since  $\pi$ -conjugated tetrazine derivatives have widespread applications in biological chemistry. Yet, this strategy is limited to the synthesis of aromatic tetrazine derivatives.

Recently, the Wu group<sup>49</sup> developed a novel strategy for the derivatization of alkyl-substituted tetrazines based on the *de novo* formation of tetrazines from nitriles and hydrazine hydrate *via* 3-mercaptopropionic acid (56) catalysis. This strategy can be used to produce tetrazine methylphosphonate derivatives from commercially available diethyl cyanomethylphosphonate (55). Furthermore,  $\pi$ -conjugated tetrazine derivatives can be synthesized *via* a Horner–Wadsworth–Emmons (HWE) reaction with tetrazine methylphosphonate (Fig. 8a). Various alkyl substituted tetrazines with excellent yields and compatibility of functional groups, such as azide (57), disulfide bond (58), alkynyl (59), amino acid (60), and glucopyranose (61), can also be synthesized using this strategy. Ditetrazine 62, which can act as a crosslink precursor in material chemistry, can also be obtained using this strategy. This strategy can also be used to develop novel fluorogenic Huaxi-Fluor probes whose efficacy was validated by the successful synthesis of pyridazine fluorophores *in situ* with large Stokes shifts and high quantum yields through the IEDDA reaction.<sup>79</sup> The IEDDA reaction between non-fluorescent probe 65 and bicyclooctyne (BCN) 63 can produce fluorescent

pyridazine with a 1273-fold turn-on ratio and large Stokes shift (212 nm). The reaction between HF<sub>645</sub> (67) and BCN (63) produced a consistently luminous product with a wide pH range (pH = 4.0 to 10.0). Furthermore, the probe 67 was also used for live-cell imaging of SKOV3 and MC3T3 cells, and *in vivo* imaging of mice bearing SKOV3 xenograft tumors (Fig. 8b).

#### 4. Derivatization of aryl tetrazines

The derivatization of aryl tetrazines provides a practical method for developing new tetrazine-substituted probes *via* C–H activation, Friedel–Crafts alkylation, and coupling reactions, which show great potential applications in bioorthogonal chemistry and materials science.

In 2015, the Audebert group<sup>69</sup> synthesized several new tetrazine-based compounds in 12–24% yields with a few substrates *via* Stille, Suzuki–Miyaura, and Hartwig–Buchwald cross-coupling reactions. In 2016, the Hierso group<sup>80</sup> reported the first efficient mono-, di-, tri-, and tetra-*ortho* C–H functionalization of 3,6-diphenyl-1,2,4,5-tetrazine (68) with moderate to excellent yields (Fig. 9a). Functional derivatizations (F, Cl, Br, I and OAc) were achieved *via* a direct Pd-catalyzed reaction under microwave irradiation at 100–120 °C in 10 min or 30 min for F functionalization and 17 h for others. The optimal yields of the products with different numbers of substituents can be achieved using different catalysts and adjusting the equivalent of functionalization reagents that act as oxidants. Pd(dba)<sub>2</sub> (dba: dibenzylidene acetone) and Pd(OAc)<sub>2</sub> were the most commonly used palladium catalysts. *N*-Fluorobenzenesulfonimide (NFSI), *N*-chlorosuccinimide (NCS), *N*-bromosuccinimide (NBS), *N*-iodosuccinimide (NIS) and PhI(OAc)<sub>2</sub> were the functionalization reagents for F, Cl, Br, I and OAc, respectively. The IEDDA reaction rate between difluorinated aryltetrazine (70a, 1 mM) and bicyclonyne dienophile (74, 1.14 eq.) in tetrahydrofuran was 0.0755 min<sup>-1</sup>, higher than that of the corresponding non-fluorinated derivative 68 (0.0355 min<sup>-1</sup>), indicating that the fluorine atoms promoted cycloaddition due to their electronic effect. Tetrazines with electron-withdrawing groups and good water solubility have high bioorthogonal reaction rates and can be used *in vivo*. Therefore, further studies are necessary to determine whether this method is compatible with electron-deficient substrates or water-soluble groups. Moreover, it will have great research value if <sup>18</sup>F functionalization can be performed in this method using [<sup>18</sup>F] NFSI, since <sup>18</sup>F is commonly used in positron emission tomography (PET).<sup>81</sup>

In 2017, the Hierso group<sup>82</sup> also reported *N*-directed Pd-catalyzed C–H *ortho*-functionalization of mono-, di-, and tetra-halogenated homofunctionalized *s*-aryltetrazines. These reactions were highly selective and efficient. The preferential halogenation sequence was from F, Cl, Br to I with a reaction time of only 10 to 45 minutes. These multihalogenated aryltetrazines could undergo halogen-selective Pd-catalyzed Suzuki–Miyaura cross-coupling reactions (Fig. 9b). For instance, 3,6-

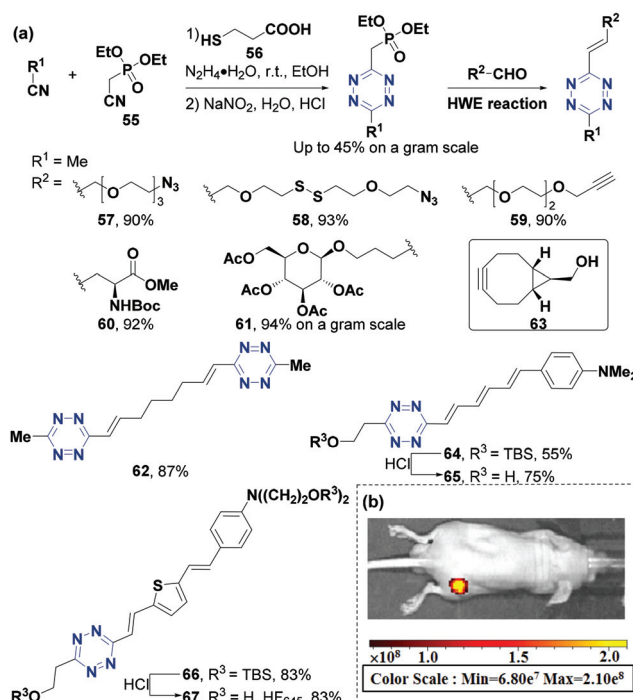
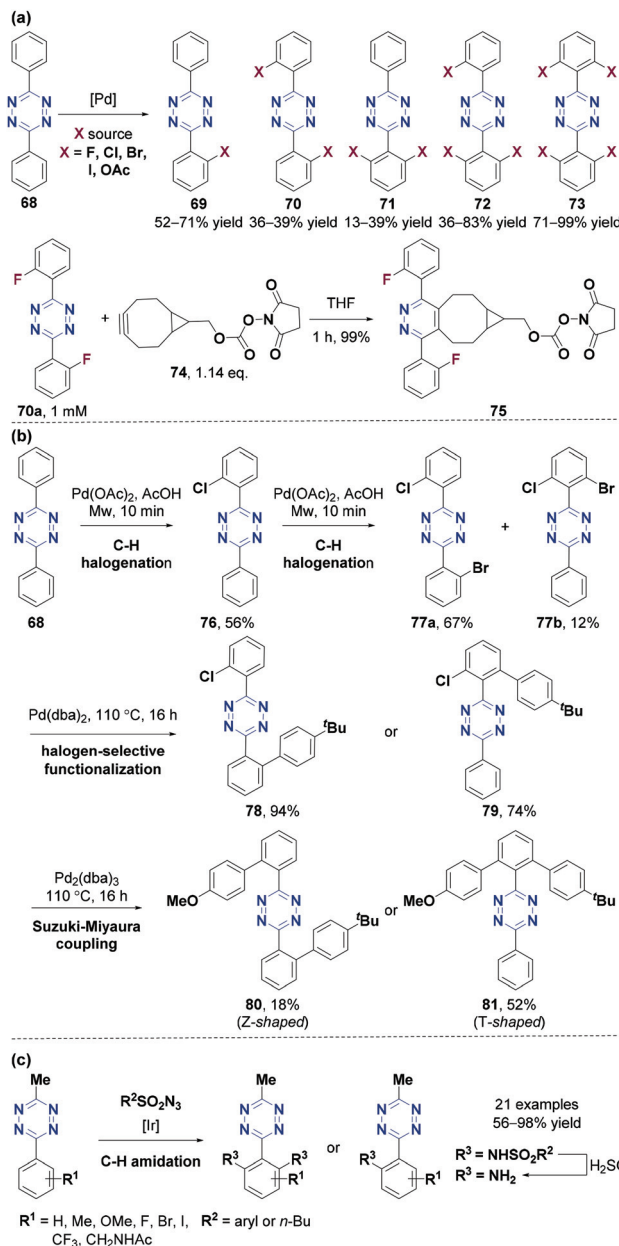


Fig. 8 Synthesis of alkyl-substituted tetrazines *via* the tetrazine–HWE reaction. (a) Synthesis method. (b) *In vivo* imaging of probe 67. (b) Adapted from ref. 79 with permission from John Wiley and Sons.



**Fig. 9** Functionalization of aryl-substituted tetrazines via C-H activation. (a) *ortho*-Functionalized aryltetrazines prepared via direct Pd-catalyzed C-H halogenation. (b) Synthesis of unsymmetrical polyhalogenated and biphenyl aryltetrazines via sequenced selective halogenation and Suzuki–Miyaura coupling reactions. (c) *ortho*-Functionalized aryltetrazines prepared via iridium-catalyzed C-H amidation.

diphenyl-1,2,4,5-tetrazine (**68**) can be halogenated from chlorination to bromination through C-H activation/halogenation, yielding dihalogenated tetrazines **77a** and **77b**. The two dihalogenated tetrazines can undergo two halogen-selective Suzuki–Miyaura cross-coupling reactions to yield polyaromatic biphenyl tetrazines **80** (Z-shaped) and **81** (T-shaped). However, 3,6-diaryltetrazine is relatively less water-soluble during bioorthogonal reactions, limiting the applications of these substrates. Besides, 3,6-diphenyltetrazine benzene with a halogen atom

can be further modified and coupled with other components. Recently, the Xu group<sup>83</sup> reported an efficient and selective iridium-catalyzed C-H amidation of 3-methyl-6-aryl-1,2,4,5-tetrazines using sulfonyl azides as amidation agents (Fig. 9c). Mono- or bis-amidation tetrazine products were selectively obtained in 56–98% yields. These compounds can be transformed into the corresponding amines *via* desulfination, which can be used either in DNA-encoded library (DEL) synthesis<sup>84</sup> or in Michael addition or nucleophilic substitution reactions to produce functional linkers for peptide rebridging, antibody–drug conjugation and live cell imaging.

Friedel–Crafts alkylation, which can attach fluorophores to aryl-substituted tetrazines, has attracted a lot of attention towards probe synthesis for biological imaging. The Vázquez group<sup>85</sup> used the general BODIPY synthesis strategy (optimized Weissleder strategy) to yield novel halogenated BODIPY-tetrazine probes (Fig. 10a). In this process, tetrazine benzyl alcohol **82** was oxidized to the tetrazine benzaldehyde derivative **83** using 2,2,6,6-tetramethylpiperidinoxy (TEMPO), thereby undergoing Friedel–Crafts alkylation with 2,4-dimethylpyrrole (**84**). BODIPY-tetrazine **85** could be produced *via* 2,3-dichloro-5,6-dicyano-1,4-benzoquinone (DDQ) oxidation. This optimized previous strategy<sup>86</sup> involved three-step reactions using hydroxymethyl benzonitrile as an initial material with a total yield of 21%. Further iodization of BODIPY-tetrazine **85** with *N*-iodosuccinimide (NIS) can produce iodinated BODIPY-tetrazine probe **86** with 96% yield. In 2019, the Wombacher group,<sup>87</sup> based on their previous work,<sup>59</sup> obtained the self-blinking (containing fluorescent quinoid and non-fluorescent spiroether isomers) fluorogenic hydroxymethyl silicon-rhodamine (f-HM-SiR) probe **89** *via* Friedel–Crafts alkylation (Fig. 10b). The fluorescence of these probes would be

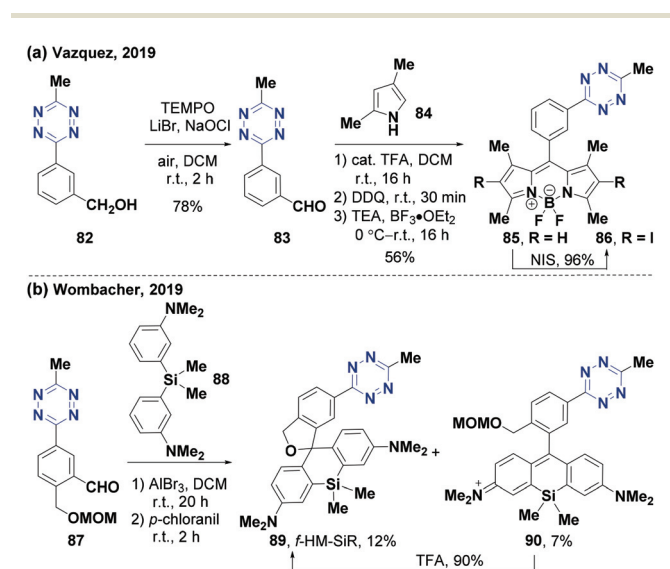


**Fig. 10** Derivatization of the aldehyde aryl-substituted tetrazine derivatives. (a) New synthesis strategy for BODIPY-tetrazine of Weissleder's probe and synthesis of the halogenated BODIPY-tetrazine derivative. (b) Synthesis of the self-blinking silicon rhodamine f-HM-SiR **89**.

quenched by through-bond energy transfer (TBET) due to the electron-withdrawing effect of the tetrazine skeleton. However, fluorescence could be turned on when the IEDDA reaction occurred. These developments and achievements demonstrated that Friedel–Crafts alkylation involving mild Lewis acids has an application prospect in tetrazine derivatization.

Aryl tetrazines with several functional groups on the aryl core have been widely used in coupling reactions to develop new tetrazine derivatives.<sup>88–90</sup> In 2020, the Hierso group<sup>91</sup> enhanced the cross-coupling of bromo-substituted aryl tetrazines by developing “doubly clickable” tetrazines *via* Cu-catalyzed coupling reactions (Fig. 11a). The constrained bis-tetrazines can undergo a double IEDDA cyclization. However, the double cycloaddition between **91** and bicyclo[6.1.0]non-4-yne (BCN, **92**) took long with 30% yield in 90 min at 20 °C in tetrahydrofuran (second-order rate constant  $k_2 = 1.45 \times 10^{-3} \text{ M}^{-1} \text{ s}^{-1}$ ). Under the same conditions, a single-ring addition

product could be obtained using a hindered BCN dienophile **93** after 90 min, due to the strong steric effect of the bridge pliers ( $k_2 = 0.47 \times 10^{-3} \text{ M}^{-1} \text{ s}^{-1}$ ). Yet, the second cycloaddition occurred above 40 °C. Therefore, these tetrazine derivatives are unlikely to be used in bioorthogonal chemistry due to the poor reaction kinetics in IEDDA reactions, but they have potential applications in materials chemistry. A series of *s*-aryltetrazines doped with O, S, N, or P was synthesized from various nucleophiles by Cu-mediated nucleophilic coupling reactions, which are difficult to obtain *via*  $S_N\text{Ar}$  reactions of halide tetrazines (Fig. 11b). In this process, triazole-tetrazines can be synthesized through click reactions from various alkynes and the azide tetrazine derivative **94** formed from azidotrimethylsilane *via* a one-pot azidation/cycloaddition strategy in 55–63% yields at 90 °C. The Huisgen azide–alkyne cycloaddition selectively occurred to form novel tetrazine derivatives with fluorophores, such as coumarin **95** and pyrene **96** (more than 50% yield). Besides, tetrazine derivatives **95** and **96** underwent IEDDA reactions with BCN **92** under the same IEDDA reaction conditions of **91** (second-order rate constant  $k_2 = 2.54 \times 10^{-2} \text{ M}^{-1} \text{ s}^{-1}$  and  $3.08 \times 10^{-2} \text{ M}^{-1} \text{ s}^{-1}$ , respectively). In 2020, the Audebert group<sup>92</sup> obtained unsymmetrical 3-monosubstituted and symmetrical tetrazines from bromo-substituted aryl tetrazines and various electron-rich aromatic secondary amines *via* Buchwald–Hartwig cross-coupling reactions (Fig. 11c). In the process, strong bases, such as  $^t\text{BuONa}$  ( $\text{p}K_a = 17$ ) and lithium hexamethyldisilamide (LHMDS,  $\text{p}K_a = 26$ ), induced the decomposition of the tetrazine core. However, the weak base  $\text{NEt}_3$  ( $\text{p}K_a = 11$ ) did not trigger any reaction. Fortunately, weak inorganic carbonate bases ( $\text{p}K_a = 10$ ), such as  $\text{K}_2\text{CO}_3$  and  $\text{Cs}_2\text{CO}_3$ , were effective in this process. Adding 4.0 equivalents of the sterically hindered ligand 2-dicyclohexylphosphino-2',4',6'-triisopropyl-biphenyl (XPhos) to the metal catalyst  $\text{Pd}_2(\text{dba})_3$  can stabilize the catalyst and hinder the binding of catalyst Pd and the tetrazine core to afford the best yields. The yield of this reaction reached 61–72%, expanding the application range of the Buchwald–Hartwig cross-coupling reaction for the functionalization of 1,2,4,5-tetrazine derivatives. Seven new donor–acceptor tetrazine analogues were synthesized under the optimized conditions, and could act as novel tetrazine-based luminescent probes for the IEDDA reaction with cyclooctyne (OCT, **101**). Monosubstituted derivatives **99a–99d** (10 mM) can undergo IEDDA reactions with OCT **101** (4.0 eq.) in dichloromethane at room temperature for a few minutes, while the reactions of 3,6-disubstituted derivatives **100a–100c** (6.7 mM) needed to be carried out at 50 °C for one hour. The two new pyridazine products of IEDDA reactions obtained between **99b** or **100b** and OCT **101** showed room-temperature phosphorescence (RTP) properties, possibly due to the phenothiazine donor attachment on the pyridazine acceptor, triggering effective intersystem crossover, thus leading to a long-lived triplet excited state.<sup>93,94</sup> RTP molecules can be used in bioimaging and sensing, organic light-emitting diodes (OLEDs) and organic photovoltaics (OPV). This Buchwald–Hartwig cross-coupling can be used to develop symmetrical and unsymmetrical tetrazines from various electron-rich aro-

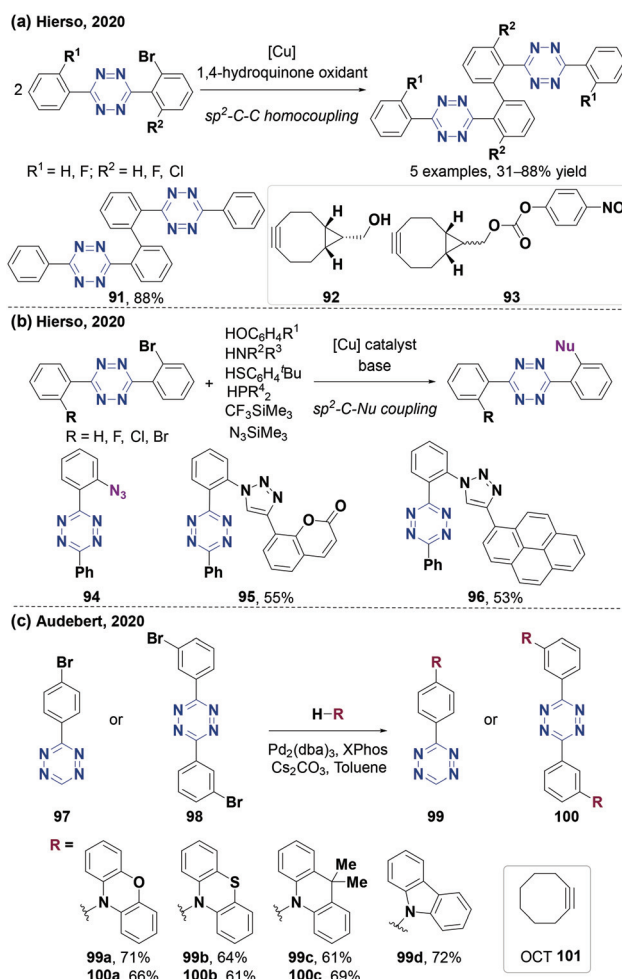


Fig. 11 Derivatization of the halogenated aryl-substituted tetrazine derivatives. (a) Synthesis of bis(tetrazine)s *via* Cu-catalyzed C–C homocoupling. (b) Derivatization of o-bromoaryl tetrazines *via* Cu-catalyzed nucleophilic coupling. (c) Functionalization of bromoaryl tetrazines *via* Buchwald–Hartwig cross-coupling.

matic secondary amines. The resulting products can be used as precursors of new functionalized tetrazines.

Metal-mediated cross-coupling reactions are widely employed in tetrazine derivatizations. Tetrazine derivatives are less reactive during coupling reactions because (1) the skeleton of tetrazine is usually unstable at high temperatures or under strong bases, (2) the multi-nitrogen core can poison the metal catalyst through coordination,<sup>95</sup> and (3) metals can reduce tetrazine and decompose the ring.<sup>96</sup> Nevertheless, great efforts and achievements have been made in the derivatization of tetrazine scaffolds for the synthesis of tetrazine derivatives and their applications in bioorthogonal chemistry.

## 5. Applications in biological chemistry

New-type synthetic methods of tetrazine derivatives have been introduced to meet the needs of chemical biology. Tetrazine-based bioorthogonal reactions are fast (kinetic constant up to  $10^7 \text{ M}^{-1} \text{ s}^{-1}$ )<sup>24</sup> with good bioorthogonality without (metal) catalysts and can be used for fluorophore conjunction to regulate fluorescence properties. Herein, the biological applications of new tetrazine probes have some distinct advantages in chemical biology, cell imaging, DNA and microRNA detection, drug release, phototherapy, and other clinical applications for disease prevention, diagnosis, and treatment.

### 5.1 Bioimaging

Bioimaging visualizes specific biomolecules at tissue, cellular, and subcellular levels, which can qualitatively and quantitat-

ively analyse biological processes in live cells by intuitively evaluating biomolecular behaviours. Probes required for effective bioimaging should have excellent biocompatibility, transmembrane ability, photobleaching resistance, high signal-to-noise ratio, and bright fluorescence. The Kele group has synthesized various tetrazine-based fluorescent probes for bioimaging based on the elimination-Heck strategy for derivatization of tetrazine developed by the Devaraj group<sup>78</sup> and Suzuki cross-coupling reaction, (Fig. 13). In 2016, they synthesized vinylene- (**102**) and phenylene-linked (**103**) phenoazazine-tetrazine probes.<sup>97</sup> The fluorescence of the probes was quenched by through-bond energy-transfer (TBET) due to the quenching effect of tetrazine. These probes could turn fluorescence on with up to 275-fold ratio when reacted with OxTCO (**111**) (Fig. 13a, **102** and **103**). These probes (5  $\mu\text{M}$ ) were also used as markers for Mammalian HEK293 T cells due to their good membrane permeability. In 2017, they used the same approach to obtain double-fluorogenic siliconrhodamine (SiR)-tetrazine probes as far-red/near-infrared dyes (**104**–**106**) for super-resolution microscopy (SRM).<sup>98</sup> Dimethylamino (**104a**, **105a** and **106a**) and diethylamino (**104b**, **105b** and **106b**) SiR-tetrazine probes had excitation maxima at around 645 nm and 655 nm and fluorescence emission occurred at around 665 nm and 670 nm, respectively, in an aqueous solution with 0.01% sodium dodecyl sulfate (SDS). These probes had rapid kinetics ( $k_2$  up to  $1923 \text{ M}^{-1} \text{ s}^{-1}$ ) and fluorescence turn-on ratio (up to 49-fold) after the IEDDA reaction with OxTCO **111** in water containing 0.1% SDS (Fig. 13a, **104**–**106**). These probes were also evaluated in bioimaging and super-resolution microscopy (SRM). The BCN<sup>endo</sup> (**112**)-modified skeletal protein vimentin<sup>116TAG</sup>-mOrange<sup>99,100</sup> (vimentin<sup>BCN<sup>endo</sup></sup>-mOrange) was used for labeling. The labeling could be observed visually in live mammalian COS-7 cells with weak background fluorescence at 37 °C for 10 minutes even at low concentrations of probes **104a** and **104b** (1.5  $\mu\text{M}$ ) (Fig. 13b). The SRM image showed higher resolution than the conventional image when **104a** was used (Fig. 13c). Recently, the Kele group also developed  $\pi$ -extended rhodamine analogs **107** to label the actin filament network from fixed COS-7 cells and skeletal protein, vimentin, from live COS-7 cells for super-resolution microscopy imaging.<sup>101</sup> In 2018, two bistetrazine-cyanines (**108a**, **108b**) (Fig. 13a) as two-point binders or cross-linker probes were synthesized<sup>102</sup> with maximum emission between 600 nm and 620 nm. The second-order rate constants ( $k_2$ ) of **108a** and **108b** with bicyclo[6.1.0]non-4-yn-9-ylmethanol (BCN, **92**) in sodium PBS containing 0.1% SDS at room temperature were  $3.1 \times 10^2 \text{ M}^{-1} \text{ s}^{-1}$  and  $1.6 \times 10^2 \text{ M}^{-1} \text{ s}^{-1}$ , respectively. Notably, the Kele group<sup>103</sup> also recently synthesized coumarinyl-tetrazine **109** through an elimination-Heck reaction, and obtained rhodol-coumarinyl-tetrazine **110** (Fig. 13a). Probe **110** was used as an activatable visible-light photocage during the IEDDA reaction in A-431 live cells to enhance the visualization of specific subcellular structures, such as mitochondria.

The synthesis of 3-substituted-6-alkenyl-*s*-tetrazines *via* the elimination-Heck approach enhances the understanding of the

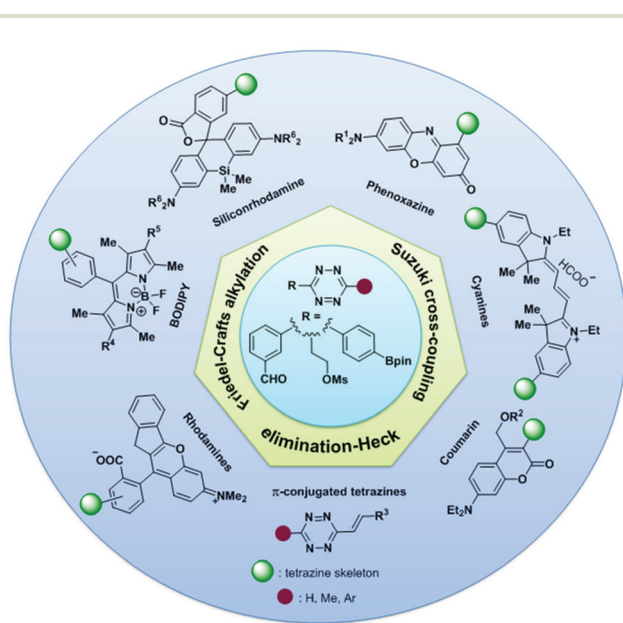
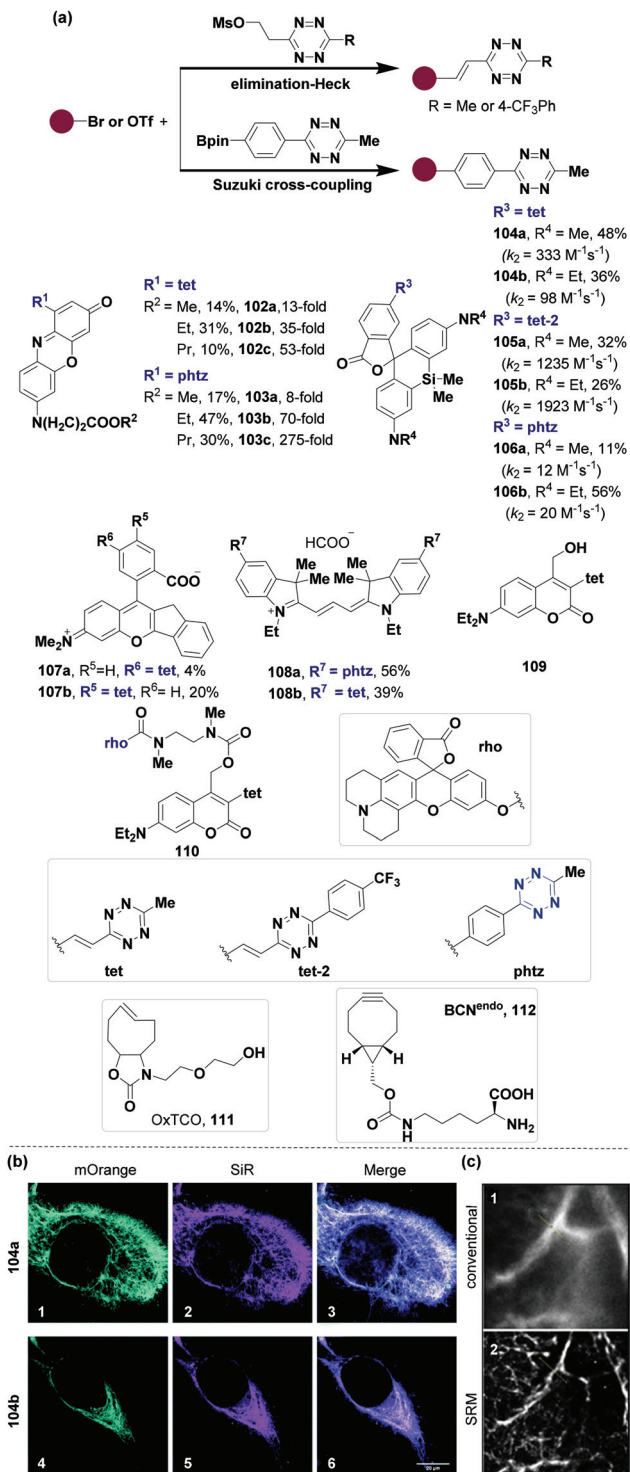
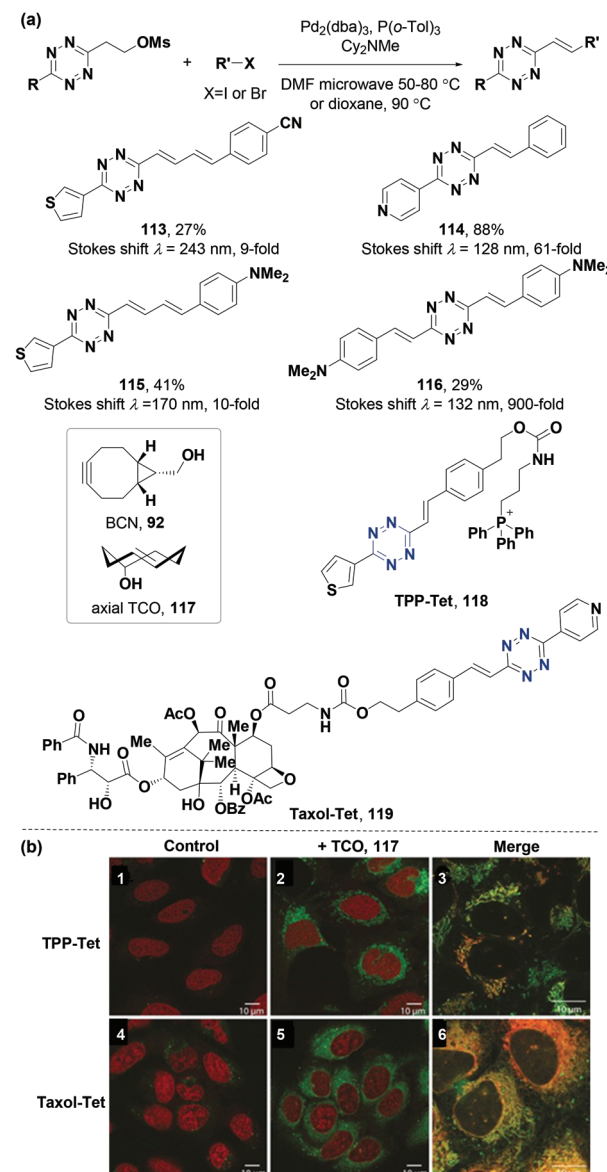


Fig. 12 Synthesis of diversified tetrazine-based probes through derivatization of the tetrazine scaffold.



**Fig. 13** Synthesis of tetrazine probes *via* elimination-Heck and Suzuki cross-coupling reactions and their applications in bioimaging. (a) Synthesis of tetrazine probes. (b) Bioimaging of SiR 104 (3  $\mu$ M) in COS-7 cells containing vimentin-BCN<sup>endo</sup>-mOrange. SiR-labeling of with dyes 104a (1, 2 and 3) and 104b (4, 5 and 6). (c) SRM images of vimentin-BCN<sup>endo</sup>-mOrange labeled with dye 104a. 1: conventional, 2: SRM. (b) and (c) Adapted from ref. 98 with permission from The Royal Society of Chemistry.

properties and potential applications of  $\pi$ -conjugated 1,2,4,5-tetrazine derivatives. The Vrabel group synthesized a series of  $\pi$ -conjugated 1,2,4,5-tetrazines (Fig. 14a) through the elimination-Heck strategy developed by the Devaraj group,<sup>78</sup> and explored their applications in labeling microtubules,<sup>104</sup> mitochondria,<sup>104–107</sup> protein of human carbonic anhydrase II (hCAII),<sup>108</sup> glycoconjugates,<sup>104,108</sup> nucleus,<sup>106</sup> and mitochondria-specific prodrug activation<sup>107</sup> in live cells of U2OS cancer cells and HeLa cells. In 2017, they demonstrated that



**Fig. 14** Construction of  $\pi$ -conjugated 1,2,4,5-tetrazines through the elimination-Heck strategy and their applications in IEDDA reactions and bioimaging. (a) Synthesis of  $\pi$ -conjugated 1,2,4,5-tetrazines and photo-physical properties of their IEDDA products. (b) Confocal micrographs of U2OS cells treated with TPP-Tet 118 or Taxol-Tet 119 (5  $\mu$ M). Nucleus was stained with DRAQ5 dye for localization. (b) Adapted from ref. 104 with permission from John Wiley and Sons.

$\pi$ -conjugated 1,2,4,5-tetrazines (0.625 mM) could undergo the IEDDA reaction with the axial TCO isomer (axially hydroxy-substituted TCO, **117**) (2.0 eq.) in  $\text{CH}_3\text{CN}$  containing 5%  $\text{H}_2\text{O}$  at room temperature for 1 hour to form fluorescent 1,4-dihydropyridazine probes *in situ* without additional fluorophore moiety attachments (Fig. 14a).<sup>104</sup> They adjusted the photochemical properties of  $\pi$ -conjugated tetrazines using different substituted groups, with maximum emission between 480 nm and 605 nm and large Stokes shifts (up to  $\lambda = 243$  nm, **113**). The second-order rate constant of this reaction was up to  $778 \text{ M}^{-1} \text{ s}^{-1}$  (**114**) in  $\text{CH}_3\text{CN}/\text{H}_2\text{O}$  1 : 3 at room temperature. Two representative  $\pi$ -conjugated 1,2,4,5-tetrazines (TPP-Tet **118** and Taxol-Tet **119**, Fig. 14a) were obtained with commendable fluorescent properties in live cells, which targeted different subcellular compartments with a tetrazine moiety (**118** in mitochondria and **119** in microtubules). Fluorescent cell labeling was performed in just a few minutes after adding TPP-Tet **118**, or Taxol-Tet **119** to U2OS live cancer cells with the treatment of axial TCO isomer **117**, indicating that the fluorescent 1,4-dihydropyridazine products of IEDDA could be efficient fluorescent labeling probes for bioimaging in live cells (Fig. 14b). A subsequent report in 2019 showed that the reaction between  $\pi$ -conjugated tetrazines (0.5 mM) containing electron-donating groups and BCN (**92**, 10 eq.) in  $\text{CH}_3\text{CN}$  at room temperature for 19 hours can *in situ*-generate pyridazine probes with large Stokes shifts (up to 170 nm for **115**) and great fluorescence enhancement turn-on ratios (up to 900-fold for **116**), indicating good bioimaging ability for mitochondria in HeLa cells and the nucleus in U2OS cells.<sup>106</sup>

With the development of tetrazine derivatization methods, more and more groups have employed novel strategies to modify tetrazine-based probes. Besides the elimination-Heck reaction, other coupling reactions have also been used to synthesize tetrazine-based probes.

The Wombacher group<sup>87</sup> first reported the fluorogenic and self-blinking properties of a tetrazine-modified f-HM-SiR derivative **89** synthesized through the Friedel-Crafts alkylation as mentioned above (Fig. 10b). This probe had several advantages including cell permeability, photostability and high brightness (extinction coefficient and quantum yield up to  $185\,000 \text{ M}^{-1} \text{ cm}^{-1}$  and 0.26, respectively), suitable for bioimaging. The fluorescence intensity of f-HM-SiR **89** was evaluated by determining the cell labeling efficacy (Fig. 15a). Fluorescence increased by 10-fold after 20 minutes of the IEDDA reaction between **89** (10  $\mu\text{M}$ ) and BCN **92** (100  $\mu\text{M}$ ) in aqueous phosphate buffers (pH 4.0, 37 °C). Moreover, the cellular labeling ability of **89** was investigated by transiently transfecting HeLa cells with histone H2A-Halo Tag and the mitochondrial import receptor subunit TOM20-HaloTag (2  $\mu\text{M}$ ) under efficient background suppression (HaloTag ligand-BCN (HTL-BCN, **120**, 10  $\mu\text{M}$ ) was targeted to the nucleus and triphenylphenyl-BCN (TPP-BCN, **121**, 10  $\mu\text{M}$ ) was targeted to mitochondria) (Fig. 15b). f-HM-SiR **89** also had good resolution imaging when used in single-molecule localization microscopy (SMLM) to image nucleus and mitochondria in live cells with simple operation (no need of high excitation power or stabiliz-

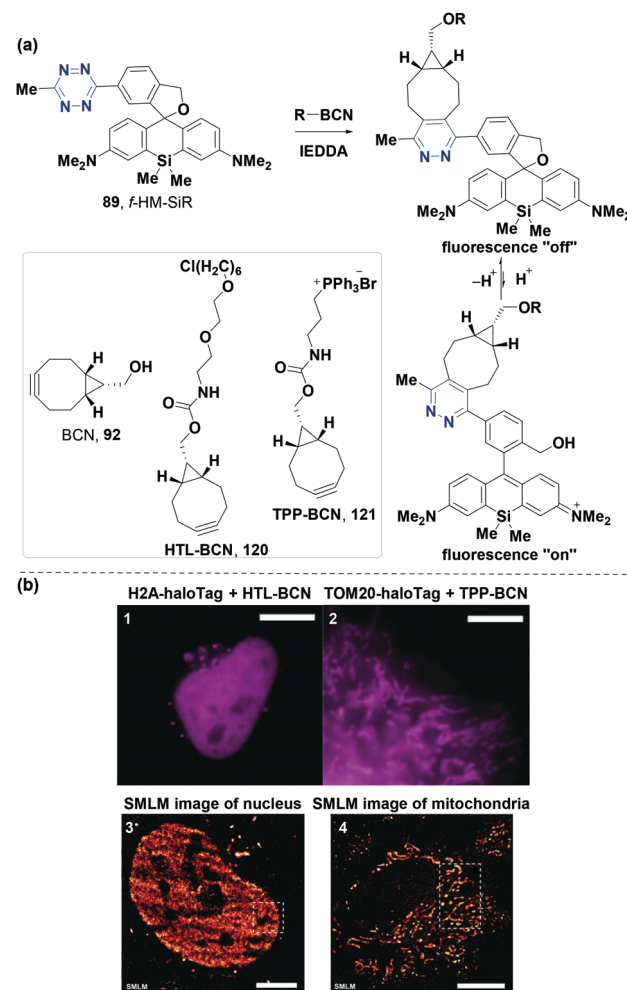


**Fig. 15** (a) Self-blinking fluorophore for the bioorthogonal IEDDA reaction. (b) Bioimaging of HeLa cells. (1) Labeling of the nucleus. (2) Labeling of mitochondria. (3) SMLM image of the nucleus. (4) SMLM image of mitochondria. Scale bars: (1, 2, 4) 10  $\mu\text{m}$  and (3) 5  $\mu\text{m}$ . (b) Adapted from ref. 87 with permission from John Wiley and Sons.

ing buffers), prolonged response time and higher spatiotemporal resolution (Fig. 15b).

## 5.2 Applications in “click-to-release” reaction

The bioorthogonal “click-to-release” reaction is a novel and effective tool used to regulate the activation of probes and prodrugs and can be used in the diagnosis and treatment of diseases.<sup>3,29,33,109–114</sup> With the deepening understanding of bioorthogonal ligation reactions, the use of biocompatible agents as bond cleavage stimuli under physiological conditions is currently a hot research topic. In addition to adding other functional groups to the biomolecules, the bioorthogonal “click-to-release” reaction provides the functional restoration of protected motifs as an ideal alternative, especially for photocages, prodrugs and masked biomolecules which are required to be bioorthogonal, non-toxic, stable, and reactive in a cellular environment. Recently, vinyl ether was explored in a “click-to-release” reaction with tetrazines to release free mole-

cules *in vitro*.<sup>109–112</sup> In 2019, the Wu group<sup>115</sup> synthesized vinyl ether-caged camptothecin (CPT) **122** as a prodrug and a tetrazine-based trigger (**123**) equipped with a near infrared (NIR) fluorophore (a Nile red derivative) based on the derivatization of the tetrazine skeleton through a Suzuki cross-coupling reaction, which was used for the “click-to-release” reaction *in vivo* (Fig. 16a). The tetrazine trigger (NR-TZ, **123**), a quenched fluorescent probe induced by the through-bond energy transfer (TBET) of tetrazine, was employed in the anti-tumor prodrug activation. The two molecules were respectively encapsulated into liposomes, which offered high plasma stability and enriched in tumors due to the enhanced permeability and retention (EPR) effect. The “click-to-release” reaction occurred

after using the two-component liposomal bioorthogonal system in a mouse model of HeLa xenograft tumors (Fig. 16a). The anticancer drug CPT (**124**) was then released to exert an anti-tumor effect and a diazine **125** was produced by the tetrazine core, resulting in significant fluorescence (about 6-fold turn-on) for imaging with byproducts of 4-(hydroxymethyl) phenol (**126**), N<sub>2</sub> and CO<sub>2</sub> (Fig. 16a and b). Therefore, the “click-to-release” reaction of the two components effectuated the generation of strong fluorescence and the release of the active drug in the aqueous medium, suggesting that the biological orthogonal “click-to-release” reaction *in vivo* has extensive application prospects, especially in tumor imaging and therapy.

Another application of the “click-to-release” reaction involving tetrazine is to detect DNA and microRNA (miRNA) templates. Many scientists have investigated the detection and imaging of nucleic acid *in situ*.<sup>116–119</sup> The Devaraj group demonstrated that tetrazine probes can be used to detect synthetic nucleic acid templates.<sup>120</sup> They also evaluated the probe efficacy in the detection of DNA and microRNA (miRNA) templates *via* a “click-to-release” reaction.<sup>121</sup> Novel tetrazine-BODIPY probes were synthesized *via* an elimination-Heck cascade reaction<sup>78</sup> between 3-mesyloxy-ethyl-6-methyltetrazine and different BODIPY derivatives.<sup>120</sup> The tetrazine-BODIPY-oligonucleotide probe (**d27'-Tz**) and dienophile 7-azabenzonorbornadiene (ABN)-oligonucleotide probe (**d27'-ABN**) were obtained from 5' and 3' amine-modified oligonucleotides. The tetrazine and dienophile accessed the desired proximity when the antisense probe was hybridized with a complementary template oligonucleotide strand (Fig. 16c). The “click-to-release” reaction occurred immediately when **d27'-Tz** (1  $\mu$ M) and **d27'-ABN** (1  $\mu$ M) were hybridized with the corresponding DNA template **d27** (1  $\mu$ M), with a 108-fold turn-on fluorescence intensity than the control reaction without **d27** after 1.5 h (a first-order rate constant of  $(9.1 \pm 0.2) \times 10^{-4} \text{ s}^{-1}$ , and a reaction half-life of 12.7 min in Tris-HCl buffer (pH = 7.4) at 25 °C). Furthermore, this strategy had good imaging and detection properties of microRNA-21 (mir-21) at low-picomolar (5 pM) levels in SKBR3 and MCF-7 breast cancer cells with significant selectivity.

### 5.3 Photodynamic therapy

Photodynamic therapy (PDT) is a promising treatment strategy for various diseases. PDT induces its effects by activating the photosensitizer through light and generating reactive oxygen species (ROS) and has many advantages, such as high selectivity, minimal invasion, exact curative effect, low toxicity, good adaptability, and reusability.<sup>122,123</sup> Notably, a photosensitizer is critical for the successful application of PDT, since its toxicity and selectivity can cause side effects. The design of a photosensitizer has been a hot research topic with great progress being achieved. However, tetrazine-based photosensitizers are rarely used in PDT. It has become facile to synthesize fluorophore-tetrazine probes due to the development of a one-pot synthesis procedure.<sup>59</sup> The Vázquez group<sup>85</sup> used this strategy to synthesize novel halogenated BODIPY-tetrazine probes

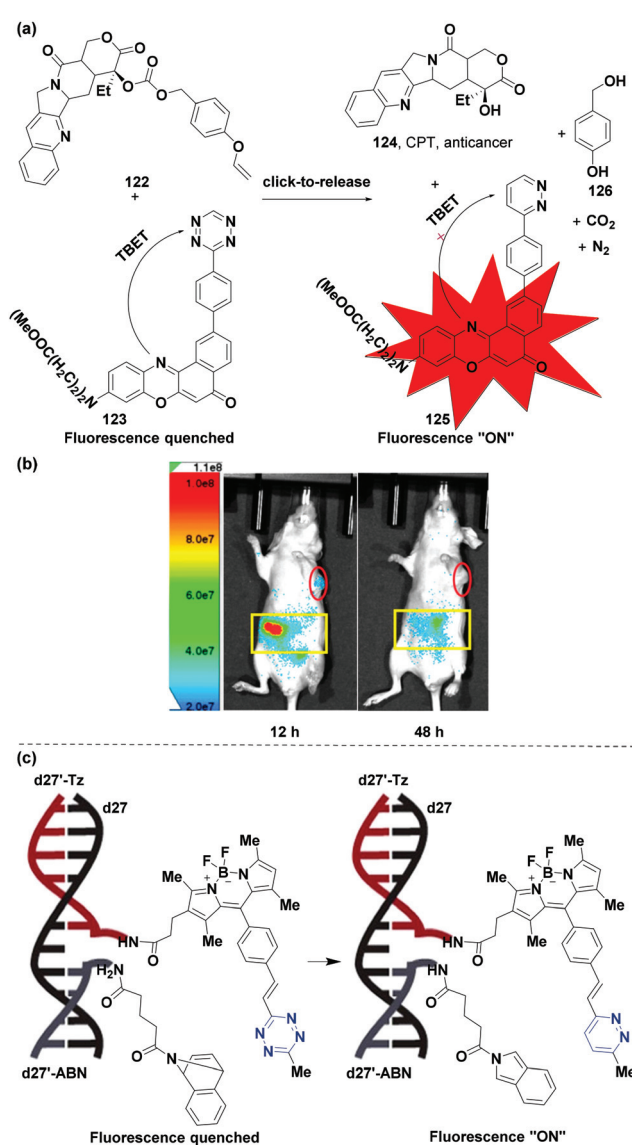
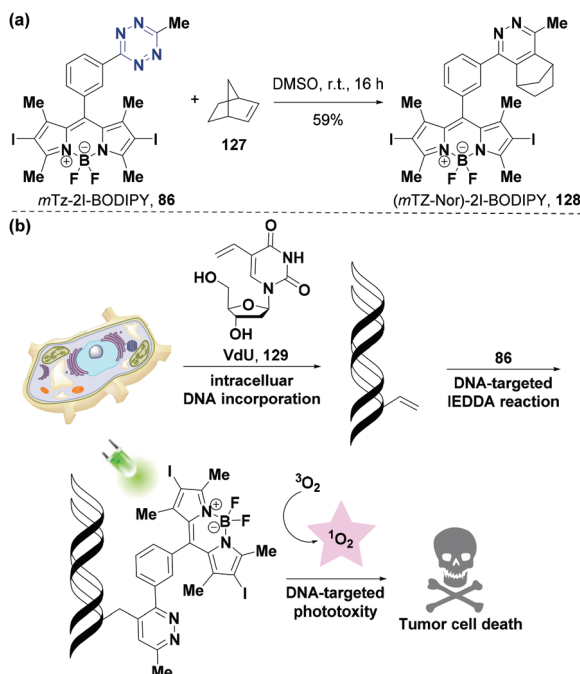


Fig. 16 Applications in “click-to-release”. (a) “Click-to-release” reaction to release CPT in tumors. (b) *In vivo* fluorescence images of tumor and abdominal regions. (c) Detection of DNA and microRNA (miRNA) templates. (b) and (c) Adapted from ref. 115 and 121 with permission from the American Chemical Society.



**Fig. 17** Application of tetrazine derivatives in PDT. (a) The IEDDA reaction between *m*Tz-2I-BODIPY 86 and norbornene 127. (b) DNA-targeted bioorthogonal strategy for PDT. (b) Adapted from ref. 85 with permission from John Wiley and Sons.

by aryl tetrazine derivatization *via* a Friedel–Crafts reaction as described above (Fig. 10a), and achieved conditional phototoxicity and specific subcellular localization in PDT through the IEDDA reaction (Fig. 17). Probe *m*Tz-2I-BODIPY (86), based on the Weissleder tetrazine-BODIPY probe, can undergo an IEDDA reaction with norbornene (127) to produce (*m*Tz-Nor)-2I-BODIPY (128) (Fig. 17a). The  $^1\text{O}_2$  quantum yield of *m*Tz-2I-BODIPY (86) ( $\Phi_\Delta = 0.217$ ) was significantly lower than that of (*m*Tz-Nor)-2I-BODIPY (128) ( $\Phi_\Delta = 0.505$ ), due to the quenching effect of tetrazine. The reaction constants for  $^1\text{O}_2$  generation of 86 and 128 were  $0.38\text{ s}^{-1}\text{10}^{-3}$  and  $2.85\text{ s}^{-1}\text{10}^{-3}$ , respectively. The cytotoxicity assay of HeLa cells showed that 86 and 128 had almost no dark toxicity (up to  $6\text{ }\mu\text{M}$ ), and 128 ( $\text{IC}_{50} = 0.212\text{ }\mu\text{M}$ ) had significant cytotoxicity (about 10-fold) than probe 86 ( $\text{IC}_{50} = 1.92\text{ }\mu\text{M}$ ) upon irradiation. The bioorthogonal IEDDA reaction between probe 86 ( $1\text{ }\mu\text{M}$ ) and dienophile 5-vinyl-2'-deoxyuridine (VdU, 129), which further caused singlet oxygen and efficient DNA damage of VdU ( $30\text{ }\mu\text{M}$ ) treated HeLa cells, showed that probe 86 was a high-efficiency photosensitizer (47% phototoxicity) (Fig. 17b). This mechanism of action is similar to that of etoposide, working as a DNA double-strand breaker agent.<sup>124</sup>

## 6. Conclusions

Tetrazines have been widely employed in the synthesis of natural products, explosive technology, coordination chemistry, material chemistry, medicinal chemistry, electro-

chemistry, and photochemistry. Tetrazines have also played critical roles in chemical biology with the rapid development of bioorthogonal chemistry. Tetrazine-based bioorthogonal reactions are crucial for cellular labeling, live-cell imaging, and disease diagnosis and treatment due to their ideal properties of chemo-selectivity, bioorthogonality, and compatibility in aqueous media. Therefore, it is necessary to determine the practical methods for tetrazine-based probe synthesis. *De novo* synthesis methods previously developed are limited by functional group compatibility or yields. Derivatization of the tetrazine skeleton or its alkyl or aryl substitutes is an alternative strategy that can be achieved *via* several reactions, such as  $\text{S}_{\text{N}}\text{Ar}$  reaction, C–H activation, Friedel–Crafts alkylation, hydrogenation, elimination–Heck reaction, Horner–Wadsworth–Emmons (HWE) reaction, and cross-coupling under Suzuki, or Stille, or Sonogashira, or Liebeskind–Srogl, or Buchwald–Hartwig conditions. Novel tetrazine probes generated *via* these synthesis reactions have shown great potential in chemical biology applications, including bioimaging, drug delivery, photodynamic therapy, and detection of DNA and microRNA. Further research studies on derivatization based on tetrazine scaffolds should focus on the development of new tetrazine coupling blocks, expansion of carbon-centered  $\text{S}_{\text{N}}\text{Ar}$  reactions and new coupling reactions that work with various substrates under mild reaction conditions, especially the synthesis of tetrazine derivatives with mono-substituents, strong electron-withdrawing functional groups or excellent water solubility. The strategy developed by the Fox group, that is, Pd-catalyzed cross-coupling and reduction reactions with easily obtained 3-thiomethyltetrazines, has excellent compatibility with functional groups and has a great application value in the future. Furthermore, selective labeling of biological macromolecules using tetrazine derivatives is essential in bioorthogonal chemistry.

## Author contributions

Haoxing Wu and Ping Feng conceived and supervised the project. Hongbao Sun summed up the literature and drafted the manuscript. Qinghe Xue and Chang Zhang proofread the manuscript. Haoxing Wu and Ping Feng revised the manuscript. All authors approved the final manuscript.

## Conflicts of interest

There are no conflicts to declare.

## Acknowledgements

This work was supported by the National Natural Science Foundation of China (21801178, 21977075), the 1.3.5 project for disciplines of excellence, West China Hospital, Sichuan University, and Post-Doctor Research Project, West China Hospital, Sichuan University (No. 2019HXBH009).

## Notes and references

1 K. Lang and J. W. Chin, Bioorthogonal Reactions for Labeling Proteins, *ACS Chem. Biol.*, 2014, **9**, 16.

2 D. M. Patterson, L. A. Nazarova and J. A. Prescher, Finding the Right (Bioorthogonal) Chemistry, *ACS Chem. Biol.*, 2014, **9**, 592.

3 B. L. Oliveira, Z. Guo and G. J. L. Bernardes, Inverse electron demand Diels–Alder reactions in chemical biology, *Chem. Soc. Rev.*, 2017, **46**, 4895.

4 T. Caneque, S. Muller and R. Rodriguez, Visualizing biologically active small molecules in cells using click chemistry, *Nat. Rev. Chem.*, 2018, **2**, 202.

5 N. K. Devaraj, The Future of Bioorthogonal Chemistry, *ACS Cent. Sci.*, 2018, **4**, 952.

6 H. Wu and N. K. Devaraj, Advances in Tetrazine Bioorthogonal Chemistry Driven by the Synthesis of Novel Tetrazines and Dienophiles, *Acc. Chem. Res.*, 2018, **51**, 1249.

7 S. S. Nguyen and J. A. Prescher, Developing bioorthogonal probes to span a spectrum of reactivities, *Nat. Rev. Chem.*, 2020, **4**, 476.

8 T. Deb, J. Tu and R. M. Franzini, Mechanisms and Substituent Effects of Metal-Free Bioorthogonal Reactions, *Chem. Rev.*, 2021, **121**, 6850.

9 S. L. Scinto, D. A. Bilodeau, R. Hincapie, W. Lee, S. S. Nguyen, M. Xu, C. W. am Ende, M. G. Finn, K. Lang, Q. Lin, J. P. Pezacki, J. A. Prescher, M. S. Robillard and J. M. Fox, Bioorthogonal chemistry, *Nat. Rev. Dis. Primers*, 2021, **1**, 30.

10 Y. Liu, R. Zeng, R. Wang, Y. Weng, R. Wang, P. Zou and P. R. Chen, Spatiotemporally resolved subcellular phosphoproteomics, *Proc. Natl. Acad. Sci. U. S. A.*, 2021, **118**, e2025299118.

11 S. Liu, C. Lin, Y. Xu, H. Luo, L. Peng, X. Zeng, H. Zheng, P. R. Chen and P. Zou, A far-red hybrid voltage indicator enabled by bioorthogonal engineering of rhodopsin on live neurons, *Nat. Chem.*, 2021, **13**, 472.

12 G. N. Lipunova, E. V. Nosova, G. V. Zyryanov, V. N. Charushin and O. N. Chupakhin, 1,2,4,5-Tetrazine derivatives as components and precursors of photo- and electroactive materials, *Org. Chem. Front.*, 2021, **8**, 5182.

13 J. Tu, M. Xu, S. Parvez, R. T. Peterson and R. M. Franzini, Bioorthogonal Removal of 3-Isocyanopropyl Groups Enables the Controlled Release of Fluorophores and Drugs in Vivo, *J. Am. Chem. Soc.*, 2018, **140**, 8410.

14 J. Tu, D. Svatunek, S. Parvez, A. C. Liu, B. J. Levandowski, H. J. Eckvahl, R. T. Peterson, K. N. Houk and R. M. Franzini, Stable, Reactive, and Orthogonal Tetrazines: Dispersion Forces Promote the Cycloaddition with Isonitriles, *Angew. Chem., Int. Ed.*, 2019, **58**, 9043.

15 J. Tu, D. Svatunek, S. Parvez, H. J. Eckvahl, M. Xu, R. T. Peterson, K. N. Houk and R. M. Franzini, Isonitrile-responsive and bioorthogonally removable tetrazine protecting groups, *Chem. Sci.*, 2020, **11**, 169.

16 T. Deb and R. M. Franzini, The Unique Bioorthogonal Chemistry of Isonitriles, *Synlett*, 2020, **31**, 938.

17 M. L. Blackman, M. Royzen and J. M. Fox, Tetrazine ligation: Fast bioconjugation based on inverse-electron-demand Diels–Alder reactivity, *J. Am. Chem. Soc.*, 2008, **130**, 13518.

18 A. Darko, S. Wallace, O. Dmitrenko, M. M. Machovina, R. A. Mehl, J. W. Chin and J. M. Fox, Conformationally strained trans-cyclooctene with improved stability and excellent reactivity in tetrazine ligation, *Chem. Sci.*, 2014, **5**, 3770.

19 N. K. Devaraj, R. Weissleder and S. A. Hilderbrand, Tetrazine-Based Cycloadditions: Application to Pretargeted Live Cell Imaging, *Bioconjugate Chem.*, 2008, **19**, 2297.

20 W. D. Lambert, S. L. Scinto, O. Dmitrenko, S. J. Boyd, R. Magboo, R. A. Mehl, J. W. Chin, J. M. Fox and S. Wallace, Computationally guided discovery of a reactive, hydrophilic trans-5-oxocene dienophile for bioorthogonal labeling, *Org. Biomol. Chem.*, 2017, **15**, 6640.

21 D. M. Patterson, L. A. Nazarova, B. Xie, D. N. Kamber and J. A. Prescher, Functionalized Cyclopropenes As Bioorthogonal Chemical Reporters, *J. Am. Chem. Soc.*, 2012, **134**, 18638.

22 R. Selvaraj and J. M. Fox, trans-Cyclooctene-a stable, voracious dienophile for bioorthogonal labeling, *Curr. Opin. Chem. Biol.*, 2013, **17**, 753.

23 M. T. Taylor, M. L. Blackman, O. Dmitrenko and J. M. Fox, Design and Synthesis of Highly Reactive Dienophiles for the Tetrazine trans-Cyclooctene Ligation, *J. Am. Chem. Soc.*, 2011, **133**, 9646.

24 Y. Fang, H. Zhang, Z. Huang, S. L. Scinto, J. C. Yang, C. W. Am Ende, O. Dmitrenko, D. S. Johnson and J. M. Fox, Photochemical syntheses, transformations, and bioorthogonal chemistry of trans-cycloheptene and sila trans-cycloheptene Ag(I) complexes, *Chem. Sci.*, 2018, **9**, 1953.

25 N. K. Devaraj, S. Hilderbrand, R. Upadhyay, R. Mazitschek and R. Weissleder, Bioorthogonal Turn-On Probes for Imaging Small Molecules inside Living Cells, *Angew. Chem., Int. Ed.*, 2010, **49**, 2869.

26 J. Li and P. R. Chen, Development and application of bond cleavage reactions in bioorthogonal chemistry, *Nat. Chem. Biol.*, 2016, **12**, 129.

27 J. M. M. Oneto, I. Khan, L. Seebald and M. Royzen, In Vivo Bioorthogonal Chemistry Enables Local Hydrogel and Systemic Pro-Drug To Treat Soft Tissue Sarcoma, *ACS Cent. Sci.*, 2016, **2**, 476.

28 R. M. Versteegen, R. Rossin, W. ten Hoeve, H. M. Janssen and M. S. Robillard, Click to Release: Instantaneous Doxorubicin Elimination upon Tetrazine Ligation, *Angew. Chem., Int. Ed.*, 2013, **52**, 14112.

29 X. Ji, Z. Pan, B. Yu, L. K. De La Cruz, Y. Zheng, B. Ke and B. Wang, Click and release: bioorthogonal approaches to “on-demand” activation of prodrugs, *Chem. Soc. Rev.*, 2019, **48**, 1077.

30 F. Lin, L. Chen, H. Zhang, W. S. C. Ngai, X. Zeng, J. Lin and P. R. Chen, Bioorthogonal Prodrug-Antibody Conjugates for On-Target and On-Demand Chemotherapy, *CCS Chem.*, 2019, **1**, 226.

31 X. Fan, Y. Ge, F. Lin, Y. Yang, G. Zhang, W. S. C. Ngai, Z. Lin, S. Zheng, J. Wang, J. Zhao, J. Li and P. R. Chen, Optimized Tetrazine Derivatives for Rapid Bioorthogonal Decaging in Living Cells, *Angew. Chem., Int. Ed.*, 2016, **55**, 14046.

32 Y. Dong, Y. Tu, K. Wang, C. Xu, Y. Yuan and J. Wang, A General Strategy for Macrotheranostic Prodrug Activation: Synergy between the Acidic Tumor Microenvironment and Bioorthogonal Chemistry, *Angew. Chem., Int. Ed.*, 2020, **59**, 7168.

33 Q. Yao, F. Lin, X. Fan, Y. Wang, Y. Liu, Z. Liu, X. Jiang, P. R. Chen and Y. Gao, Synergistic enzymatic and bioorthogonal reactions for selective prodrug activation in living systems, *Nat. Commun.*, 2018, **9**, 5032.

34 H. S. Han, E. Niemeyer, Y. Huang, W. S. Kamoun, J. D. Martin, J. Bhaumik, Y. Chen, S. Roberge, J. Cui, M. R. Martin, D. Fukumura, R. K. Jain, M. G. Bawendi and D. G. Duda, Quantum dot/antibody conjugates for in vivo cytometric imaging in mice, *Proc. Natl. Acad. Sci. U. S. A.*, 2015, **112**, 1350.

35 H. S. Jang, S. Jana, R. J. Blizzard, J. C. Meeuwsen and R. A. Mehl, Access to Faster Eukaryotic Cell Labeling with Encoded Tetrazine Amino Acids, *J. Am. Chem. Soc.*, 2020, **142**, 7245.

36 S. V. Mayer, A. Murnauer, M. K. von Wrisberg, M. L. Jokisch and K. Lang, Photo-induced and Rapid Labeling of Tetrazine-Bearing Proteins via Cyclopropenone-Caged Bicyclononynes, *Angew. Chem., Int. Ed.*, 2019, **58**, 15876.

37 X. Li, Z. Liu and S. Dong, Bicyclo[6.1.0]nonyne and tetrazine amino acids for Diels–Alder reactions, *RSC Adv.*, 2017, **7**, 44470.

38 B. M. Zeglis, K. K. Sevak, T. Reiner, P. Mohindra, S. D. Carlin, P. Zanzonico, R. Weissleder and J. S. Lewis, A Pretargeted PET Imaging Strategy Based on Bioorthogonal Diels–Alder Click Chemistry, *J. Nucl. Med.*, 2013, **54**, 1389.

39 W. Wei, Z. T. Rosenkrans, J. Liu, G. Huang, Q.-Y. Luo and W. Cai, Immuno PET: Concept, Design, and Applications, *Chem. Rev.*, 2020, **120**, 3787.

40 R. Rossin, P. R. Verkerk, S. M. van den Bosch, R. C. M. Vulders, I. Verel, J. Lub and M. S. Robillard, In Vivo Chemistry for Pretargeted Tumor Imaging in Live Mice, *Angew. Chem., Int. Ed.*, 2010, **49**, 3375.

41 S. M. van Duijnhoven, R. Rossin, S. M. van den Bosch, M. P. Wheatcroft, P. J. Hudson and M. S. Robillard, Diabody Pretargeting with Click Chemistry In Vivo, *J. Nucl. Med.*, 2015, **56**, 1422.

42 E. M. F. Billaud, S. Belderbos, F. Cleeren, W. Maes, M. Van de Wouwer, M. Koole, A. Verbruggen, U. Himmelreich, N. Geukens and G. Bormans, Pretargeted PET Imaging Using a Bioorthogonal <sup>18</sup>F-Labeled trans-Cyclooctene in an Ovarian Carcinoma Model, *Bioconjugate Chem.*, 2017, **28**, 2915.

43 X. Shi, K. Gao, H. Huang and R. Gao, Pretargeted Immuno-PET Based on Bioorthogonal Chemistry for Imaging EGFR Positive Colorectal Cancer, *Bioconjugate Chem.*, 2018, **29**, 250.

44 E. Ruivo, F. Elvas, K. Adhikari, C. Vangestel, G. Van Haesendonck, F. Lemière, S. Staelens, S. Stroobants, P. Van der Veken, L. Wyffels and K. Augustyns, Preclinical Evaluation of a Novel <sup>18</sup>F-Labeled dTCO-Amide Derivative for Bioorthogonal Pretargeted Positron Emission Tomography Imaging, *ACS Omega*, 2020, **5**, 4449.

45 A. Pinner, Ueber die Einwirkung von Hydrazin auf Imidoäther, *Ber. Dtsch. Chem. Ges.*, 1893, **26**, 2126.

46 G. Clavier and P. Audebert, s-Tetrazines as Building Blocks for New Functional Molecules and Molecular Materials, *Chem. Rev.*, 2010, **110**, 3299.

47 J. Yang, M. R. Karver, W. Li, S. Sahu and N. K. Devaraj, Metal-catalyzed one-pot synthesis of tetrazines directly from aliphatic nitriles and hydrazine, *Angew. Chem., Int. Ed.*, 2012, **51**, 5222.

48 Y. Qu, F. X. Sauvage, G. Clavier, F. Miomandre and P. Audebert, Metal-Free Synthetic Approach to 3-Monosubstituted Unsymmetrical 1,2,4,5-Tetrazines Useful for Bioorthogonal Reactions, *Angew. Chem., Int. Ed.*, 2018, **57**, 12057.

49 W. Mao, W. Shi, J. Li, D. Su, X. Wang, L. Zhang, L. Pan, X. Wu and H. Wu, Organocatalytic and Scalable Syntheses of Unsymmetrical 1,2,4,5-Tetrazines by Thiol-Containing Promotors, *Angew. Chem., Int. Ed.*, 2019, **58**, 1106.

50 Z. Fang, W.-L. Hu, D.-Y. Liu, C.-Y. Yu and X.-G. Hu, Synthesis of tetrazines from gem-difluoroalkenes under aerobic conditions at room temperature, *Green Chem.*, 2017, **19**, 1299.

51 H. H. Szmant, The Mechanism of the Wolff-Kishner Reduction, Elimination, and Isomerization Reactions, *Angew. Chem., Int. Ed. Engl.*, 1968, **7**, 120.

52 J. Faragó, Z. Novák, G. Schlosser, A. Csámpai and A. Kotschy, The azaphilic addition of organometallic reagents on tetrazines: scope and limitations, *Tetrahedron*, 2004, **60**, 1991.

53 Q. Zhou, P. Audebert, G. Clavier, F. Miomandre and J. Tang, New unsymmetrical alkyl-s-tetrazines: original syntheses, fluorescence and electrochemical behaviour, *RSC Adv.*, 2014, **4**, 7193.

54 Z. Novák and A. Kotschy, First cross-coupling reactions on tetrazines, *Org. Lett.*, 2003, **5**, 3495.

55 N. Leconte, A. Keromnes-Wuillaume, F. Suzenet and G. Guillaumet, Efficient Palladium-Catalyzed Synthesis of Unsymmetrical (Het)aryl-tetrazines, *Synlett*, 2007, 0204.

56 A. M. Bender, T. C. Chopko, T. M. Bridges and C. W. Lindsley, Preparation of Unsymmetrical 1,2,4,5-Tetrazines via a Mild Suzuki Cross-Coupling Reaction, *Org. Lett.*, 2017, **19**, 5693.

57 J. M. Contreras, Y. M. Rival, S. Chayer, J. J. Bourguignon and C. G. Wermuth, Aminopyridazines as acetylcholinesterase inhibitors, *J. Med. Chem.*, 1999, **42**, 730.

58 R. J. Blizzard, D. R. Backus, W. Brown, C. G. Bazewicz, Y. Li and R. A. Mehl, Ideal Bioorthogonal Reactions Using A Site-Specifically Encoded Tetrazine Amino Acid, *J. Am. Chem. Soc.*, 2015, **137**, 10044.

59 A. Wieczorek, P. Werther, J. Euchner and R. Wombacher, Green- to far-red-emitting fluorogenic tetrazine probes-synthetic access and no-wash protein imaging inside living cells, *Chem. Sci.*, 2017, **8**, 1506.

60 F. Pop, J. Ding, L. M. L. Daku, A. Hauser and N. Avarvari, Tetrathiafulvalene-s-tetrazine: versatile platform for donor-acceptor systems and multifunctional ligands, *RSC Adv.*, 2013, **3**, 3218.

61 E. Ros, A. Prades, D. Forson, J. Smyth, X. Verdaguer, L. R. d. Pouplana and A. Riera, Synthesis of 3-alkyl-6-methyl-1,2,4,5-tetrazines via a Sonogashira-type cross-coupling reaction, *Chem. Commun.*, 2020, **56**, 11086.

62 A. Maggi, E. Ruivo, J. Fissers, C. Vangestel, S. Chatterjee, J. Joossens, F. Sobott, S. Staelens, S. Stroobants, P. Van Der Veken, L. Wyffels and K. Augustyns, Development of a novel antibody-tetrazine conjugate for bioorthogonal pre-targeting, *Org. Biomol. Chem.*, 2016, **14**, 7544.

63 A. Counotte-Potman, H. C. Van der Plas, B. Van Veldhuizen and C. A. Landheer, Occurrence of the SN (ANRORC) mechanism in the hydrazination of 1,2,4,5-tetrazines, *J. Org. Chem.*, 1981, **46**, 5102.

64 S. D. Schnell, L. V. Hoff, A. Panchagnula, M. H. H. Wurzenberger, T. M. Klapötke, S. Sieber, A. Linden and K. Gademann, 3-Bromotetrazine: labelling of macromolecules via monosubstituted bifunctional s-tetrazines, *Chem. Sci.*, 2020, **11**, 3042.

65 D. E. Chavez and M. A. Hiskey, Synthesis of the bi-heterocyclic parent ring system 1,2,4-triazolo[4,3-b][1,2,4,5]tetrazine and some 3,6-disubstituted derivatives, *J. Heterocycl. Chem.*, 1998, **35**, 1329.

66 J. Zhu, J. Hiltz, R. B. Lennox and R. Schirrmacher, Chemical modification of single walled carbon nanotubes with tetrazine-tethered gold nanoparticles via a Diels-Alder reaction, *Chem. Commun.*, 2013, **49**, 10275.

67 E. Ros, M. Bellido, X. Verdaguer, L. Ribas de Pouplana and A. Riera, Synthesis and Application of 3-Bromo-1,2,4,5-Tetrazine for Protein Labeling to Trigger Click-to-Release Bioorthogonal Reactions, *Bioconjugate Chem.*, 2020, **31**, 933.

68 L. V. Hoff, S. D. Schnell, A. Tomio, A. Linden and K. Gademann, Cross-Coupling Reactions of Monosubstituted Tetrazines, *Org. Lett.*, 2021, **23**, 5689.

69 C. Quinton, V. Alain-Rizzo, C. Dumas-Verdes, G. Clavier, L. Vignau and P. Audebert, Triphenylamine/tetrazine based  $\pi$ -conjugated systems as molecular donors for organic solar cells, *New J. Chem.*, 2015, **39**, 9700.

70 W. D. Lambert, Y. Z. Fang, S. Mahapatra, Z. Huang, C. W. A. Ende and J. M. Fox, Installation of Minimal Tetrazines through Silver-Mediated Liebeskind-Srogl Coupling with Arylboronic Acids, *J. Am. Chem. Soc.*, 2019, **141**, 17068.

71 J. F. Hooper, R. D. Young, I. Pernik, A. S. Weller and M. C. Willis, Carbon-carbon bond construction using boronic acids and aryl methyl sulfides: orthogonal reactivity in Suzuki-type couplings, *Chem. Sci.*, 2013, **4**, 1568.

72 F. Pan, H. Wang, P. X. Shen, J. Zhao and Z. J. Shi, Cross coupling of thioethers with aryl boroxines to construct biaryls via Rh catalyzed C-S activation, *Chem. Sci.*, 2013, **4**, 1573.

73 J. C. T. Carlson, L. G. Meimetis, S. A. Hilderbrand and R. Weissleder, BODIPY-Tetrazine Derivatives as Superbright Bioorthogonal Turn-on Probes, *Angew. Chem., Int. Ed.*, 2013, **52**, 6917.

74 M. R. Karver, R. Weissleder and S. A. Hilderbrand, Synthesis and Evaluation of a Series of 1,2,4,5-Tetrazines for Bioorthogonal Conjugation, *Bioconjugate Chem.*, 2011, **22**, 2263.

75 C. R. Butler, E. M. Beck, A. Harris, Z. Huang, L. A. McAllister, C. W. A. Ende, K. Fennell, T. L. Foley, K. Fonseca, S. J. Hawrylik, D. S. Johnson, J. D. Knaefels, S. Mente, G. S. Noell, J. Pandit, T. B. Phillips, J. R. Piro, B. N. Rogers, T. A. Samad, J. E. Wang, S. Y. Wan and M. A. Brodney, Azetidine and Piperidine Carbamates as Efficient, Covalent Inhibitors of Monoacylglycerol Lipase, *J. Med. Chem.*, 2017, **60**, 9860.

76 J. W. Chang, M. J. Niphakis, K. M. Lum, A. B. Cognetta 3rd, C. Wang, M. L. Matthews, S. Niessen, M. W. Buczynski, L. H. Parsons and B. F. Cravatt, Highly selective inhibitors of monoacylglycerol lipase bearing a reactive group that is bioisosteric with endocannabinoid substrates, *Chem. Biol.*, 2012, **19**, 579.

77 Y. Xie, Y. Fang, Z. Huang, A. M. Tallon, C. W. Am Ende and J. M. Fox, Divergent Synthesis of Monosubstituted and Unsymmetrical 3,6-Disubstituted Tetrazines from Carboxylic Ester Precursors, *Angew. Chem., Int. Ed.*, 2020, **59**, 16967.

78 H. Wu, J. Yang, J. Šečkuté and N. K. Devaraj, In situ synthesis of alkenyl tetrazines for highly fluorogenic bioorthogonal live-cell imaging probes, *Angew. Chem., Int. Ed.*, 2014, **53**, 5805.

79 W. Mao, J. Tang, L. Dai, X. He, J. Li, L. Cai, P. Liao, R. Jiang, J. Zhou and H. Wu, A General Strategy to Design Highly Fluorogenic Far-Red and Near-Infrared Tetrazine Bioorthogonal Probes, *Angew. Chem., Int. Ed.*, 2021, **60**, 2393.

80 C. Testa, E. Gigot, S. Genc, R. Decreau, J. Roger and J. C. Hierso, Ortho-Functionalized Aryltetrazines by Direct Palladium-Catalyzed C-H Halogenation: Application to Fast Electrophilic Fluorination Reactions, *Angew. Chem., Int. Ed.*, 2016, **55**, 5555.

81 S. Preshlock, M. Tredwell and V. Gouverneur,  $^{18}\text{F}$ -Labeling of Arenes and Heteroarenes for Applications in Positron Emission Tomography, *Chem. Rev.*, 2016, **116**, 719.

82 C. D. Mboyi, C. Testa, S. Reeb, S. Genc, H. Cattey, P. Fleurat-Lessard, J. Roger and J. C. Hierso, Building Diversity in ortho-Substituted s-Aryltetrazines By Tuning N-Directed Palladium C-H Halogenation: Unsymmetrical

Polyhalogenated and Biphenyl s-Aryltetrazines, *ACS Catal.*, 2017, **7**, 8493.

83 H. Xiong, Y. Gu, S. Zhang, F. Lu, Q. Ji, L. Liu, P. Ma, G. Yang, W. Hou and H. Xu, Iridium-catalyzed C–H amidation of s-tetrazines, *Chem. Commun.*, 2020, **56**, 4692.

84 H. Xu, F. Ma, N. Wang, W. Hou, H. Xiong, F. Lu, J. Li, S. Wang, P. Ma, G. Yang and R. A. Lerner, DNA-Encoded Libraries: Aryl Fluorosulfonates as Versatile Electrophiles Enabling Facile On-DNA Suzuki, Sonogashira, and Buchwald Reactions, *Adv. Sci.*, 2019, **6**, 1901551.

85 G. Linden, L. Zhang, F. Pieck, U. Linne, D. Kosenkov, R. Tonner and O. Vazquez, Conditional Singlet Oxygen Generation through a Bioorthogonal DNA-targeted Tetrazine Reaction, *Angew. Chem., Int. Ed.*, 2019, **58**, 12868.

86 J. C. Carlson, L. G. Meimetis, S. A. Hilderbrand and R. Weissleder, BODIPY-tetrazine derivatives as superbright bioorthogonal turn-on probes, *Angew. Chem., Int. Ed.*, 2013, **52**, 6917.

87 P. Werther, K. Yserentant, F. Braun, N. Kaltwasser, C. Popp, M. Baalmann, D. P. Herten and R. Wombacher, Live-Cell Localization Microscopy with a Fluorogenic and Self-Blinking Tetrazine Probe, *Angew. Chem., Int. Ed.*, 2020, **59**, 804.

88 A. Wieczorek, T. Buckup and R. Wombacher, Rigid tetrazine fluorophore conjugates with fluorogenic properties in the inverse electron demand Diels–Alder reaction, *Org. Biomol. Chem.*, 2014, **12**, 4177.

89 Y. Lee, W. Cho, J. Sung, E. Kim and S. B. Park, Monochromophoric Design Strategy for Tetrazine-Based Colorful Bioorthogonal Probes with a Single Fluorescent Core Skeleton, *J. Am. Chem. Soc.*, 2018, **140**, 974.

90 L. Peng, Y. Yu, J. Lu, P. He, G. Wang, M. Huang, B. Zhao, Y. Pei and S. Tan, Development of s-tetrazine-based polymers for efficient polymer solar cells by controlling appropriate molecular aggregation, *Dyes Pigm.*, 2019, **171**, 107717.

91 C. D. Mboyi, D. Vivier, A. Daher, P. Fleurat-Lessard, H. Cattey, C. H. Devillers, C. Bernhard, F. Denat, J. Roger and J. C. Hierso, Bridge-Clamp Bis(tetrazine)s with  $[N]_8$   $\pi$ -Stacking Interactions and Azido-s-Aryl Tetrazines: Two Classes of Doubly Clickable Tetrazines, *Angew. Chem., Int. Ed.*, 2020, **59**, 1149.

92 Y. Qu, P. Pander, O. Vybornyi, M. Vasylieva, R. Guillot, F. Miomandre, F. B. Dias, P. Skabara, P. Data, G. Clavier and P. Audebert, Donor–Acceptor 1,2,4,5-Tetrazines Prepared by the Buchwald–Hartwig Cross-Coupling Reaction and Their Photoluminescence Turn-On Property by Inverse Electron Demand Diels–Alder Reaction, *J. Org. Chem.*, 2020, **85**, 3407.

93 P. Pander, A. Swist, R. Motyka, J. Soloducho, F. B. Dias and P. Data, Thermally activated delayed fluorescence with a narrow emission spectrum and organic room temperature phosphorescence by controlling spin-orbit coupling and phosphorescence lifetime of metal-free organic molecules, *J. Mater. Chem. C*, 2018, **6**, 5434.

94 P. Pander, A. Swist, J. Soloducho and F. B. Dias, Room temperature phosphorescence lifetime and spectrum tuning of substituted thianthrenes, *Dyes Pigm.*, 2017, **142**, 315.

95 W. Kaim, The coordination chemistry of 1,2,4,5-tetrazines, *Coord. Chem. Rev.*, 2002, **230**, 127.

96 S. Maji, B. Sarkar, S. Patra, J. Fiedler, S. M. Mobin, V. G. Puranik, W. Kaim and G. K. Lahiri, Metal-induced reductive ring opening of 1,2,4,5-tetrazines: three resulting coordination alternatives, including the new non-innocent 1,2-diiminohydrazido(2-) bridging ligand system, *Inorg. Chem.*, 2006, **45**, 1316.

97 G. Knorr, E. Kozma, A. Herner, E. A. Lemke and P. Kele, New Red-Emitting Tetrazine-Phenoxazine Fluorogenic Labels for Live-Cell Intracellular Bioorthogonal Labeling Schemes, *Chem. – Eur. J.*, 2016, **22**, 8972.

98 E. Kozma, G. E. Girona, G. Paci, E. A. Lemke and P. Kele, Bioorthogonal double-fluorogenic siliconrhodamine probes for intracellular super-resolution microscopy, *Chem. Commun.*, 2017, **53**, 6696.

99 C. Uttamapinant, J. D. Howe, K. Lang, V. Beránek, L. Davis, M. Mahesh, N. P. Barry and J. W. Chin, Genetic Code Expansion Enables Live-Cell and Super-Resolution Imaging of Site-Specifically Labeled Cellular Proteins, *J. Am. Chem. Soc.*, 2015, **137**, 4602.

100 I. Nikić, G. Estrada Girona, J. H. Kang, G. Paci, S. Mikhaleva, C. Koehler, N. V. Shymanska, C. Ventura Santos, D. Spitz and E. A. Lemke, Debugging Eukaryotic Genetic Code Expansion for Site-Specific Click-PAINT Super-Resolution Microscopy, *Angew. Chem., Int. Ed.*, 2016, **55**, 16172.

101 A. Egyed, A. Kormos, B. Soveges, K. Nemeth and P. Kele, Bioorthogonally applicable,  $\pi$ -extended rhodamines for super-resolution microscopy imaging for intracellular proteins, *Bioorg. Med. Chem.*, 2020, **28**, 115218.

102 A. Kormos, C. Koehler, E. A. Fodor, Z. R. Rutkai, M. E. Martin, G. Mezo, E. A. Lemke and P. Kele, Bistetrazine-Cyanines as Double-Clicking Fluorogenic Two-Point Binder or Crosslinker Probes, *Chem. – Eur. J.*, 2018, **24**, 8841.

103 M. Bojtár, K. Németh, F. Domahidy, G. Knorr, A. Verkman, M. Kállay and P. Kele, Conditionally Activatable Visible-Light Photocages, *J. Am. Chem. Soc.*, 2020, **142**, 15164.

104 A. Vázquez, R. Dzijak, M. Dračínský, R. Rampmaier, S. J. Siegl and M. Vrabel, Mechanism-Based Fluorogenic trans-Cyclooctene-Tetrazine Cycloaddition, *Angew. Chem., Int. Ed.*, 2017, **56**, 1334.

105 S. J. Siegl, J. Galeta, R. Dzijak, A. Vázquez, M. Del Río-Villanueva, M. Dračínský and M. Vrabel, An Extended Approach for the Development of Fluorogenic trans-Cyclooctene-Tetrazine Cycloadditions, *ChemBioChem*, 2019, **20**, 886.

106 S. J. Siegl, J. Galeta, R. Dzijak, M. Dračínský and M. Vrabel, Bioorthogonal Fluorescence Turn-On Labeling Based on Bicyclononyne-Tetrazine Cycloaddition

Reactions that Form Pyridazine Products, *ChemPlusChem*, 2019, **84**, 493.

107 R. Dzijak, J. Galeta, A. Vázquez, J. Kozák, M. Matoušová, H. Fulka, M. Dračínský and M. Vrabel, Structurally Redesigned Bioorthogonal Reagents for Mitochondria-Specific Prodrug Activation, *JACS Au*, 2020, **1**, 23.

108 S. J. Siegl, A. Vázquez, R. Dzijak, M. Dračínský, J. Galeta, R. Rampmaier, B. Klepetářová and M. Vrabel, Design and Synthesis of Aza-Bicyclononene Dienophiles for Rapid Fluorogenic Ligations, *Chem. – Eur. J.*, 2018, **24**, 2426.

109 H. Wu, S. C. Alexander, S. Jin and N. K. Devaraj, A Bioorthogonal Near-Infrared Fluorogenic Probe for mRNA Detection, *J. Am. Chem. Soc.*, 2016, **138**, 11429.

110 E. Jiménez-Moreno, Z. Guo, B. L. Oliveira, I. S. Albuquerque, A. Kitowski, A. Guerreiro, O. Boutureira, T. Rodrigues, G. Jiménez-Osés and G. J. L. Bernardes, Vinyl Ether/Tetrazine Pair for the Traceless Release of Alcohols in Cells, *Angew. Chem., Int. Ed.*, 2017, **56**, 243.

111 K. Neumann, A. Gambardella, A. Lilienkampf and M. Bradley, Tetrazine-mediated bioorthogonal prodrug-prodrug activation, *Chem. Sci.*, 2018, **9**, 7198.

112 L. P. W. M. Lelieveldt, S. Eising, A. Wijen and K. M. Bonger, Vinylboronic acid-caged prodrug activation using click-to-release tetrazine ligation, *Org. Biomol. Chem.*, 2019, **17**, 8816.

113 J. C. T. Carlson, H. Mikula and R. Weissleder, Unraveling Tetrazine-Triggered Bioorthogonal Elimination Enables Chemical Tools for Ultrafast Release and Universal Cleavage, *J. Am. Chem. Soc.*, 2018, **140**, 3603.

114 A. H. A. M. van Onzen, R. M. Versteegen, F. J. M. Hoeben, I. A. W. Filot, R. Rossin, T. Zhu, J. Wu, P. J. Hudson, H. M. Janssen, W. Ten Hoeve and M. S. Robillard, Bioorthogonal Tetrazine Carbamate Cleavage by Highly Reactive trans-Cyclooctene, *J. Am. Chem. Soc.*, 2020, **142**, 10955.

115 X. Xie, B. W. Li, J. Wang, C. Y. Zhan, Y. Huang, F. Zeng and S. Z. Wu, Bioorthogonal Nanosystem for Near-Infrared Fluorescence Imaging and Prodrug Activation in Mouse Model, *ACS Mater. Lett.*, 2019, **1**, 549.

116 S. Kummer, A. Knoll, E. Socher, L. Bethge, A. Herrmann and O. Seitz, Fluorescence Imaging of Influenza H1N1 mRNA in Living Infected Cells Using Single-Chromophore FIT-PNA, *Angew. Chem., Int. Ed.*, 2011, **50**, 1931.

117 A. Okamoto, ECHO probes: a concept of fluorescence control for practical nucleic acid sensing, *Chem. Soc. Rev.*, 2011, **40**, 5815.

118 S. Sando and E. T. Kool, Imaging of RNA in bacteria with self-ligating quenched probes, *J. Am. Chem. Soc.*, 2002, **124**, 9686.

119 S. Tyagi and F. R. Kramer, Molecular beacons: Probes that fluoresce upon hybridization, *Nat. Biotechnol.*, 1996, **14**, 303.

120 J. Seckute, J. Yang and N. K. Devaraj, Rapid oligonucleotide-templated fluorogenic tetrazine ligations, *Nucleic Acids Res.*, 2013, **41**, e148.

121 H. Wu, B. T. Cisneros, C. M. Cole and N. K. Devaraj, Bioorthogonal Tetrazine-Mediated Transfer Reactions Facilitate Reaction Turnover in Nucleic Acid-Tern plated Detection of MicroRNA, *J. Am. Chem. Soc.*, 2014, **136**, 17942.

122 R. Ackroyd, C. Kelty, N. Brown and M. Reed, The history of photodetection and photodynamic therapy, *Photochem. Photobiol.*, 2001, **74**, 656.

123 D. E. J. G. J. Dolmans, D. Fukumura and R. K. Jain, Photodynamic therapy for cancer, *Nat. Rev. Cancer*, 2003, **3**, 380.

124 A. Montecucco, F. Zanetta and G. Biamonti, Molecular Mechanisms of Etoposide, *EXCLI J.*, 2015, **14**, 95.